

# Thiabicyclononane-based Antimicrobial Polycations

Zhishuai Geng, M.G. Finn\*

School of Chemistry & Biochemistry, Georgia Institute of Technology, 901 Atlantic Dr., Atlanta,  
GA 30332, USA

E-mail: mgfinn@gatech.edu

## Supporting Information

### Table of contents

Additional Background .....	2
General Materials and Methods .....	2
Instrumentation .....	2
Synthesis and characterization of new compounds .....	3
Modeling of polymer structure .....	4
Characterization of BCN polymers .....	5
Critical micelle concentration (CMC) measurement .....	8
DNA binding .....	9
Measurement of antimicrobial activity .....	9
Measurements of hemolytic activity .....	10
Evidence for membrane disruption .....	11
Measurements of antimicrobial resistance .....	11
Surface modification and characterization .....	12
Antimicrobial control experiments for surface modified with covalently-attached <b>3b</b> .....	13
Repeat antimicrobial activity without washing .....	14
Harsher washing conditions for reuse of derivatized glass .....	15
Antimicrobial activity towards <i>B. subtilis</i> and <i>P. aeruginosa</i> .....	16
Mammalian cell viability in contact with derivatized glass chips .....	16
Scanning electron microscopy (SEM) measurements .....	16
NMR Spectra .....	17
References .....	30

## **Additional Background**

Resistance mechanisms to cationic agents include modifications of the external surface of the bacterium<sup>1,2</sup> (including changes in capsular polysaccharide,<sup>3,4</sup> outer membrane proteins,<sup>5,6</sup> and other membrane adhesion systems<sup>7</sup>), proteolytic attack on the antimicrobial peptide,<sup>8,9</sup> and upregulation of transporters.<sup>10</sup> Small quaternary ammonium compounds have been similarly touted as being difficult to generate resistance against, but this, too, is proving to be incorrect.<sup>11</sup> Nevertheless, oligomeric and polymeric cationic species are usually assumed to target bacterial membranes and, because they can be engineered to resist some of the natural defense mechanisms, still represent a promising approach toward antimicrobial applications.

## **General Materials and Methods**

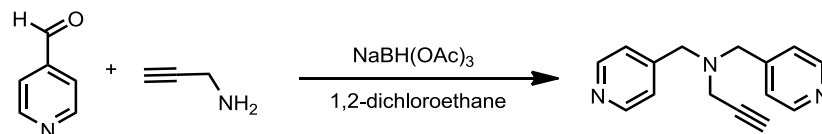
Reagents and solvents were purchased from commercial sources and used as received, unless otherwise stated. When dry solvents were required, solvents were passed through activated alumina columns on an MBraun solvent purification system (MB-SPS), collected in oven-dried glassware prior to use and stored under inert atmosphere with molecular sieves inside. Water was purified on a Millipore Milli-Q Advantage A10 system. Unless otherwise stated, the reactions were performed under inert atmosphere in capped reaction vessels. Flash chromatography was performed on 60-mesh silica. Analytical TLC was performed on aluminum-backed plates and visualized by exposure to UV light and/or staining with aqueous potassium permanganate (2%  $\text{KMnO}_4$  + 5%  $\text{K}_2\text{CO}_3$ ).

## **Instrumentation**

NMR spectra were obtained on Bruker AMX-400, and DRX-500 instruments in deuterated solvents (Cambridge Isotope Laboratories, Inc.) and referenced to the signals of residual protons in the NMR solvent. Spectra were processed in MestReNova software (Mestrelab Research). Routine mass spectra were obtained on an Advion Compact Mass Spectrometer (G1946D) ESI-MSD instrument, using direct sample injection followed with 9:1  $\text{CH}_3\text{CN}:\text{H}_2\text{O}$  containing 0.1% formic acid as mobile phase. UV-vis absorbance spectra was collected on a VarioskanFlash plate reader (ThermoFisher). Gel permeation chromatography (GPC) analysis was performed in water/methanol/glacial acetic acid (volume percentage 54/23/23), 0.5M NaOAc, at 0.8 mL/min flow rate (LC-20AD pump) on a Shimadzu GPC setup equipped with two Ultrahydrogel 10  $\mu\text{m}$  linear columns (300 x 7.8 mm), autosampler (SIL-20A) and column oven (CTO-20A) set at 40 °C. Detection was achieved using a diode array detector (SPD-M20A), and RI detector (RID-10A), and instrument was calibrated with Dextran kit (Phenomenex ALO-2772). Dynamic light scattering measurements were taken on a DynaPro plate reader and analyzed with Dynamics® software (Wyatt Technology, Santa Barbara, CA). The XPS data were recorded using a Thermo K-Alpha spectrometer with an Al-K $\alpha$  source. Static contact angle measurements were taken on a ramé-hart contact angle goniometer using a 1 mL drop of 18 MW water (pH 7).

## Synthesis and characterization of new compounds

*Representative procedure for the synthesis of bispyridine linker (2b, 2c, 2d, and 2h)*



4-pyridinecarboxaldehyde (1.71 g, 16 mmol) and propargylamine (330 mg, 6 mmol) (or respective amine for other bispyridine linkers) were mixed in 1,2-dichloroethane (60 mL) and then treated with sodium triacetoxyborohydride (4.24 g, 20 mmol). The mixture was stirred at room temperature under N<sub>2</sub> atmosphere for overnight. The reaction mixture was quenched by adding aqueous saturated NaHCO<sub>3</sub>, and the product was extracted with dichloromethane, dried (MgSO<sub>4</sub>) and purified by column chromatography (1:1%:0.5% dichloromethane/methanol/triethylamine) elution. The desired product **2b** was obtained as a pale yellow liquid (978 mg, 70% yield). <sup>1</sup>H NMR (500 MHz, CDCl<sub>3</sub>) δ 8.58 (d, *J* = 5.9 Hz, 4H), 7.35 (d, *J* = 5.9 Hz, 4H), 3.71 (s, 4H), 3.29 (d, *J* = 2.3 Hz, 1H), 2.33 (t, *J* = 2.3 Hz, 1H). <sup>13</sup>C NMR (126 MHz, CDCl<sub>3</sub>) δ 149.73, 147.34, 123.56, 77.10, 74.08, 56.34, 41.61.

**2c**, yellow liquid (70% yield). <sup>1</sup>H NMR (500 MHz, CDCl<sub>3</sub>) δ 8.58 (s, 4H), 7.32 (s, 4H), 5.59 (s, 1H), 3.54 (s, 4H), 3.20 (dd, *J* = 13.4, 6.9 Hz, 2H), 2.44 – 2.36 (m, 2H), 2.20 – 2.10 (m, 4H), 1.94 (t, *J* = 2.6 Hz, 1H), 1.67 – 1.56 (m, 2H), 1.56 – 1.41 (m, 6H), 1.41 – 1.33 (m, 2H), 1.33 – 1.19 (m, 10H). <sup>13</sup>C NMR (126 MHz, CDCl<sub>3</sub>) δ 173.16, 149.85, 148.82, 123.85, 84.81, 77.41, 77.16, 76.91, 68.21, 57.67, 54.05, 39.46, 36.92, 29.77, 29.32, 29.28, 29.01, 28.74, 28.50, 27.11, 26.92, 26.82, 25.85, 18.45.

**2d**, yellow liquid (70% yield). <sup>1</sup>H NMR (500 MHz, CDCl<sub>3</sub>) δ 8.48 (d, *J* = 5.6 Hz, 4H), 7.22 (d, *J* = 5.6 Hz, 4H), 3.50 (s, 4H), 3.24 (t, *J* = 6.7 Hz, 2H), 2.45 (t, *J* = 6.9 Hz, 2H), 1.84 – 1.58 (m, 2H). <sup>13</sup>C NMR (126 MHz, CDCl<sub>3</sub>) δ 149.64, 147.93, 123.29, 57.33, 50.86, 48.96, 26.25.

**2e**, **2f** and **2g** were made from **2s** and respective azide under the catalysis of 5 mol% of copper sulfate pentahydrate and 10 mol% of sodium ascorbate in 4:1 of H<sub>2</sub>O/*t*-BuOH mixture overnight and then purified by column chromatography (elution with CH<sub>2</sub>Cl<sub>2</sub> containing 1% MeOH and 0.5% Et<sub>3</sub>N).

**2e**, yellow liquid (70% yield). <sup>1</sup>H NMR (400 MHz, CDCl<sub>3</sub>) δ 8.58 (s, 4H), 7.40 (s, 1H), 7.35 (s, 4H), 4.33 (t, *J* = 7.3 Hz, 2H), 3.75 (s, 2H), 3.63 (s, 4H), 1.98 – 1.71 (m, 2H), 1.42 – 1.12 (m, 10H), 0.85 (t, *J* = 6.8 Hz, 1H). <sup>13</sup>C NMR (126 MHz, CDCl<sub>3</sub>) δ 149.76, 147.93, 143.78, 123.40, 122.12, 56.65, 50.22, 48.09, 31.50, 30.14, 28.88, 28.75, 26.33, 22.41, 17.61, 13.88.

**2f**, yellow liquid (70% yield). <sup>1</sup>H NMR (500 MHz, CDCl<sub>3</sub>) δ 8.56 (s, 4H), 7.39 (s, 1H), 7.34 (s, 4H), 4.34 (dd, *J* = 9.6, 4.8 Hz, 2H), 3.76 (s, 2H), 3.65 (s, 4H), 1.89 (s, 2H), 1.27 (d, *J* = 32.7 Hz, 26H), 0.87 (t, *J* = 7.8, 5.6 Hz, 3H). <sup>13</sup>C NMR (101 MHz, CDCl<sub>3</sub>) δ 149.94, 148.05, 143.91, 123.55, 122.31, 56.82, 50.37, 48.24, 31.90, 30.30, 29.66, 29.63, 29.58, 29.49, 29.39, 29.34, 28.97, 26.50, 22.67, 14.11.

**2g**, white powder (70% yield). <sup>1</sup>H NMR (500 MHz, CDCl<sub>3</sub>) δ 8.59 (d, *J* = 3.1 Hz, 4H), 7.59 (s,

1H), 7.37 (d,  $J = 5.3$  Hz, 4H), 5.40 (d,  $J = 3.7$  Hz, 1H), 5.17 (s, 2H), 4.73 (tdd,  $J = 34.9, 19.9, 15.4$  Hz, 2H), 3.82 (s, 2H), 3.68 (s, 4H), 2.36 (d,  $J = 7.8$  Hz, 2H), 2.01 (ddd,  $J = 22.0, 9.7, 4.2$  Hz, 2H), 1.93 – 1.86 (m, 2H), 1.86 – 1.80 (m, 1H), 1.68 – 1.59 (m, 6H), 1.57 – 1.44 (m, 4H), 1.36 (dd,  $J = 11.4, 6.1$  Hz, 2H), 1.28 (d,  $J = 7.8$  Hz, 2H), 1.23 – 1.06 (m, 6H), 1.01 (d,  $J = 8.2$  Hz, 3H), 0.93 (d,  $J = 6.5$  Hz, 3H), 0.90 – 0.85 (m, 6H), 0.70 (s, 3H).  $^{13}\text{C}$  NMR (126 MHz,  $\text{CDCl}_3$ )  $\delta$  165.49, 149.82, 147.79, 144.19, 138.66, 123.86, 123.42, 123.25, 56.56, 56.47, 55.93, 50.87, 49.77, 47.87, 42.12, 39.49, 39.33, 37.75, 36.62, 36.34, 35.99, 35.60, 31.69, 31.62, 28.03, 27.84, 27.48, 24.09, 23.64, 22.64, 22.38, 20.84, 19.07, 18.53, 11.67.

**2h**, brown liquid (70% yield).  $^1\text{H}$  NMR (400 MHz,  $\text{CDCl}_3$ )  $\delta$  8.57 (d,  $J = 6.0$  Hz, 4H), 7.33 (d,  $J = 6.0$  Hz, 4H), 3.66 (s, 4H), 2.62 (dd,  $J = 8.3, 5.9$  Hz, 2H), 2.49 (dd,  $J = 8.1, 5.8$  Hz, 2H), 2.21 (s, 6H).  $^{13}\text{C}$  NMR (101 MHz,  $\text{CDCl}_3$ )  $\delta$  149.78, 148.54, 123.49, 57.92, 57.66, 52.07, 45.79.

**2j**,  $^1\text{H}$  NMR (400 MHz,  $\text{CDCl}_3$ )  $\delta$  8.83 (d,  $J = 1.5$  Hz, 2H), 8.49 (d,  $J = 2.9$  Hz, 2H), 7.79 (dd,  $J = 2.9, 1.7$  Hz, 2H), 4.28 (t,  $J = 6.0$  Hz, 4H), 3.95 (s, 6H), 2.36 (dt,  $J = 12.1, 6.1$  Hz, 2H).

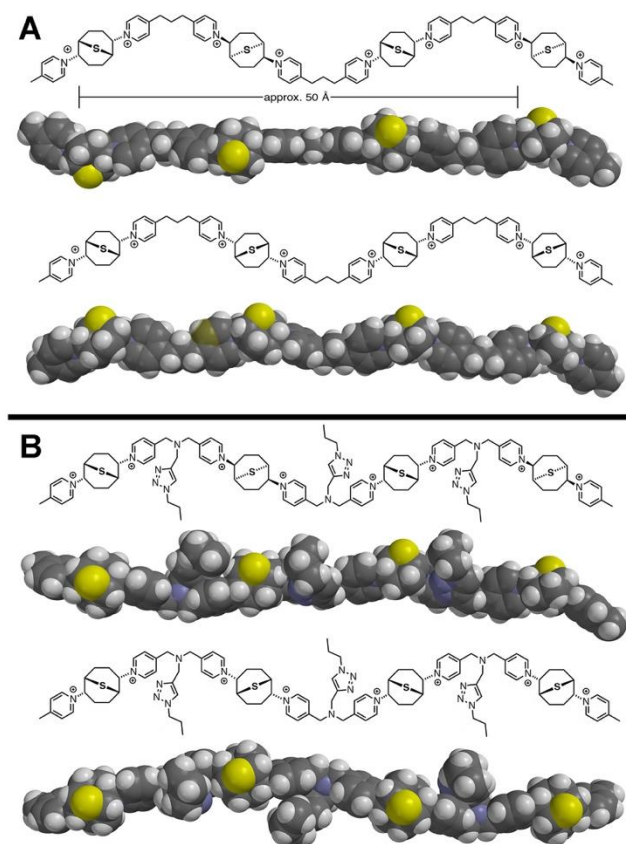
#### *Representative procedure for the synthesis of polymers.*

Compound **1a** (21 mg, 0.1 mmol, 1 equiv), silver nitrate (34 mg, 0.2 mmol, 2 equiv) and the bispyridine of interest (0.1 mmol, 1 equiv) were mixed in 0.5 mL DMSO and stirred overnight at room temperature under inert atmosphere. After centrifugation, any solid material was filtered out and the resulting solution was added to 15 mL  $\text{CH}_2\text{Cl}_2$  or toluene (for very hydrophobic polycations such as **3f** and **3g**) to precipitate the desired product. The material was isolated by filtration and dried to give a yellow sticky solid.

#### **Modeling of polymer structure**

Tetrameric analogues of **3a** were minimized by simple molecular mechanics calculation (MMFF force field, no solvent) in Spartan 16, using Monte Carlo surveying of available conformations. Energy-minimized structures are shown in Figure S1, which are approximately 17 Å long per repeat unit.

**Figure S1.** Energy-minimized model structures of oligomeric analogues of (A) **3a** and (B) **3e**, the latter with a propyl group on each triazole rather than an octyl group to simplify the calculation. For each set, structures having bicyclononane units of the same (top) and alternating (bottom) chirality are shown. Molecular mechanics calculations were performed with Spartan16 without consideration of counterion or solvent contributions. We expect the synthesized polymers to contain random sequences in terms of diastereomeric composition of diad, triad, or larger substructures.



## Characterization of BCN polymers

Average chain lengths were determined by end-group analysis using  $^1\text{H}$  NMR. Gel permeation chromatography (GPC) analysis in a high-ionic strength ternary composition aqueous-based mobile phase was also performed to provide a rough estimation of relative sizes (Figure S2, Table S1), but was less trustworthy for absolute molecular weight determination due to the lack of an appropriate standard and the likelihood of interactions between the polymers and the stationary phase, a well-known phenomenon for polyelectrolytes.<sup>12</sup> The polymers were also characterized by dynamic light scattering (DLS) in a plate reader, also noted in Table S1.

*Gel permeation chromatography.* Three BCN based polymers were dissolved at 0.8 mg/mL concentration in a 54/23/23 (v/v/v %) mixture of water/methanol/acetic acid, containing 0.5M NaOAc solution (conditions used in published reports<sup>12,13</sup>) and characterized by aqueous gel permeation chromatography (GPC, black curves in Figure S2). The major peaks between 17 and 30 mins were assigned to polymers. Calculation of molecular weight parameters by comparison to PEI standards proved to be nonsensical, so  $M_n$ ,  $M_w$ , and polydispersities were evaluated by comparison to PEG (for the low molecular weight range) and PEI (high molecular weight range) standards. We regard NMR end group analysis as the most accurate method available to us.

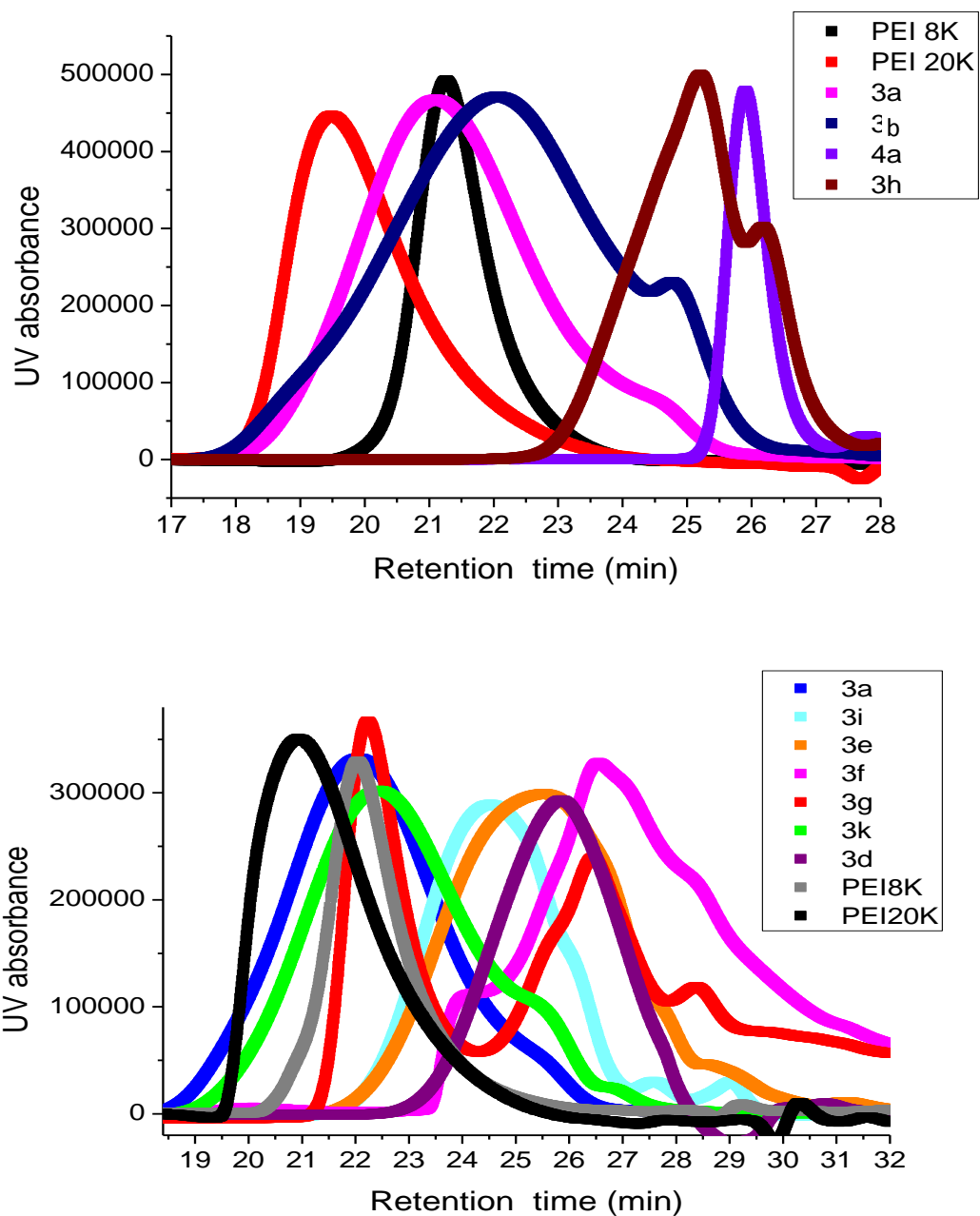


**Figure S2.** GPC curves of BCN polycations and PEI standards in 54/23/23 (v/v/v %) water/methanol/acetic acid, 0.5M NaOAc.

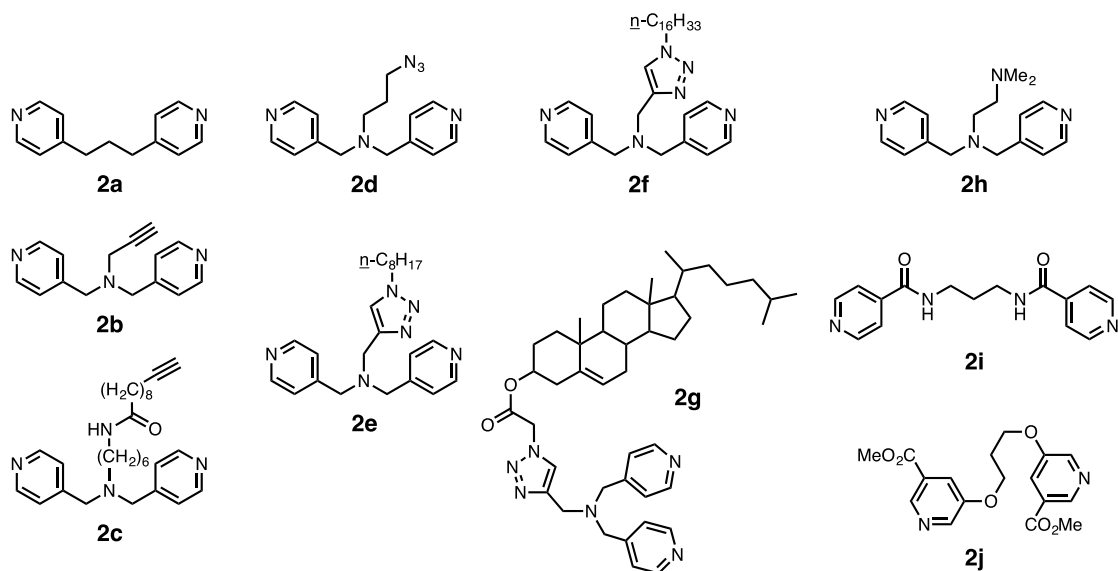


**Table S1.** Characterization of polycations by  $^1\text{H}$  NMR, GPC, and DLS. DLS was performed on polymer solutions of 1 mg/mL in 54/23/23 (v/v/v %) water/methanol/acetic acid, containing 0.5M NaOAc, “n/o” denotes a sample for which no signal for an aggregate was observed. “n/d” = not determined.

polymer	$M_n$ (Da) <sup>a</sup>	$M_n$ (Da) <sup>b</sup>	PDI <sup>b</sup>	$R_h$ (nm) <sup>c</sup>	polydisp. (%) <sup>c</sup>
<b>3a</b>	9200	11000	1.36	$101 \pm 10$	19.6
<b>3b</b>	6200	n/d	n/d	$77 \pm 4$	14.7
<b>3d</b>	5500	1250	1.5	$35 \pm 5$	45.2
<b>3e</b>	5300	1400	2.04	n/d	n/d
<b>3f</b>	6100	4000	1.03	n/o	n/o
<b>3g</b>	11600	9000	1.07	$14 \pm 1$	10.2
<b>3h</b>	1600	n/d	n/d	$87 \pm 6$	13.8
<b>3i</b>	8800	3000	1.4	$151 \pm 12$	10.8
<b>3j</b>	11000	n/d	n/d	$82 \pm 5$	15.9
<b>3k</b>	8400	n/d	n/d	$111 \pm 11$	12.3
PEI	8000	n/d	n/d	$5 \pm 1$	26.8

(a) by  $^1\text{H}$  NMR. (b) by GPC. (c) Hydrodynamic radius and polydispersity measured by DLS in the same solvent as GPC.

## Critical micelle concentration (CMC) measurement.

CMC values were determined by measurement of the conductivity of a polymer solution at various concentrations in deionized water (starting conductivity < 1  $\mu\text{S}/\text{cm}$ ). Figure S3 shows representative data for **3a**, **3e**, and cetyltrimethylammonium bromide (CTAB) as a positive control. The observed CMC (defined as the break point between linear conductivity-vs.-concentration plots) for CTAB (310  $\mu\text{g}/\text{mL}$ ) was consistent with literature values (330-350  $\mu\text{g}/\text{mL}$  at 0.92-1 mM).<sup>14</sup> The polymers showed no break point in this analysis up to the maximum value able to be measured by the instrument, and therefore we assume that micelles are not formed by these compounds in the concentration ranges of 1-400  $\mu\text{g}/\text{mL}$  for **3a**, and 1-64  $\mu\text{g}/\text{mL}$  for **3e**, both of which are 10 times higher than their MIC<sub>90</sub> towards *E.coli*.

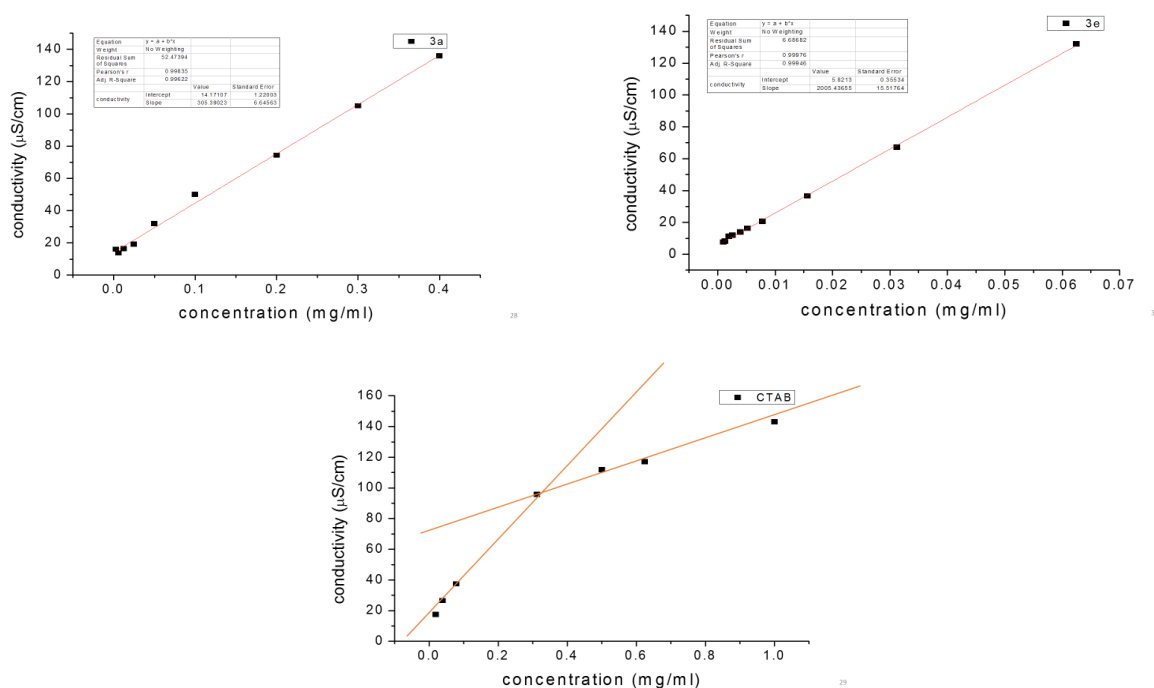


**Figure S3.** CMC determined by conductivity-concentration plots for **3a**, **3e** and CTAB.



## DNA binding

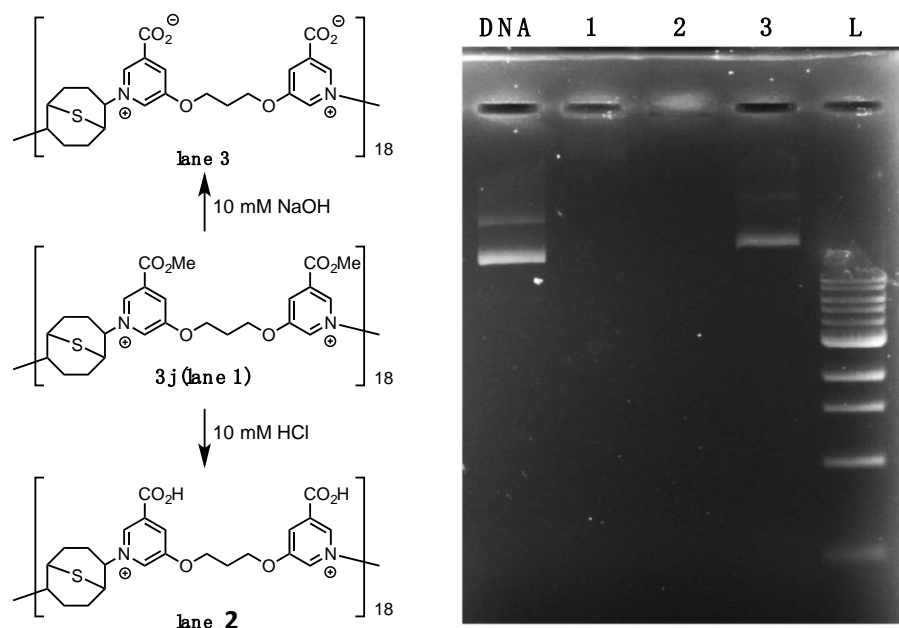


**Figure S4.** Efficiency of condensing DNA by **3j**, after **3j** had been treated with water (lane 1), HCl (lane 2), or NaOH (lane 3). Each mixture contained DNA at 50  $\mu\text{g/mL}$  and **3j** at 1.6  $\text{mg/mL}$  (N:P = 40).

## Measurement of antimicrobial activity

Bacteria suspensions (*E. coli* and *B. subtilis* subsp. *subtilis* (Ehrenberg) Cohn (ATCC® 6051™)) were grown in Mueller-Hinton Broth (MHB) overnight at 37 °C. The resulting culture was used to inoculate a second culture in 2 mL of MHB medium until an optical density of 0.8 at 600 nm was reached.

**Method A.** The suspension was diluted with fresh MHB to an optical density at 600 nm ( $\text{OD}_{600}$ ) of approximately 0.001. This suspension was mixed with different concentrations of freshly prepared polymer solutions in TRIS saline (pH 7.0) in a 96-well plate, and incubated overnight at 37 °C. The  $\text{OD}_{600}$  was measured for bacteria suspensions that were incubated in the presence vs. absence of polymer. Antibacterial activity was expressed as minimal inhibitory concentration (MIC), the concentration at which more than 90% inhibition of growth was observed. All experiments were performed in triplicate.

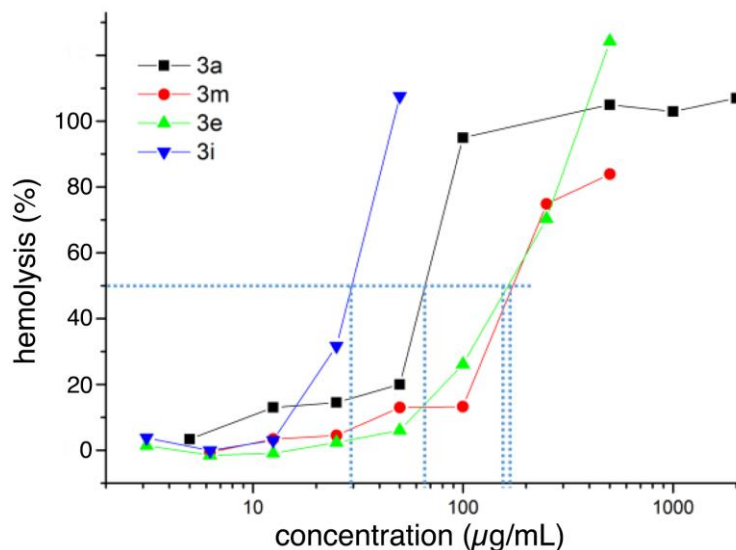
**Method B.** The bacteria were collected by centrifugation at 4,000  $\times g$  for 3 min at 4 °C, washed with sterile PBS (pH 7.4) and suspended in PBS to a final concentration of  $6 \times 10^6$  cells  $\text{mL}^{-1}$ . The glass/silicon substrate (0.01-0.04  $\text{cm}^2$  in area) or polymer solution was added to 50  $\mu\text{L}$  of the bacterial suspension and gently shaken for 0.5-4 hours. Then 25  $\mu\text{L}$  of suspension was spread onto a sterile Petri dish covered with a layer of LB medium containing 0.8% agar (previously autoclaved,

and cooled to 37 °C). After overnight incubation at 37 °C, bacterial colonies became visible and were counted and compared with the untreated bacteria plate. The MIC was defined as the minimum concentration in the diluted series when the CFU number on the agar plate reached no more than 10% of the control plate.

### Measurements of hemolytic activity

These were performed by a standard method,<sup>15</sup> with slight modifications. Freshly drawn human red blood cells (RBCs) were obtained by centrifuging a whole blood at 300g for 7 minutes (no brake) to remove plasma and white blood cells. A sample of the resulting RBC suspension (100  $\mu$ L) was diluted with 3.9 mL TBS buffer (10 mM Tris buffer, pH = 7.0, 150 mM NaCl) to give a stock suspension of 0.25% RBCs. This stock (120  $\mu$ L), TBS buffer (15  $\mu$ L) and the polymer stock solutions (15  $\mu$ L) (or control solutions) were added to a 1.5 mL tube and incubated at 37°C for 1 hour. The tube was centrifuged at 10,000 rpm for 5 minutes. The supernatant (60  $\mu$ L) was transferred to a 96-well plate and hemolysis detected by measurement of absorbance of the released hemoglobin at 414 nm. 100% Hemolysis was obtained by adding 15  $\mu$ L of Triton-X100 solution to sample RBC suspensions while 0% hemolysis was defined as the absorbance from suspension treated with TBS containing no polymer. A dilution series of polycation gave the HC<sub>50</sub> value by linear interpolation of concentration inducing 50% hemolysis, as illustrated in the examples in Figure S5. All experiments were run in triplicate.

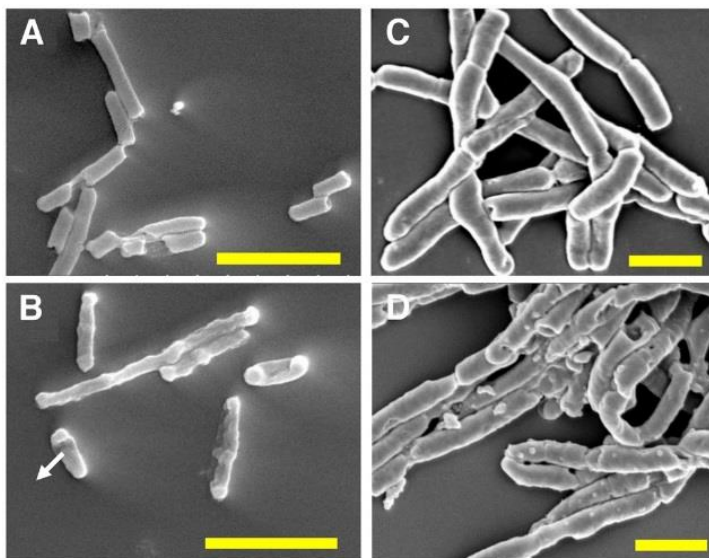
**Figure S5.** Representative hemolytic profiles of BCN polycations; this experiment was performed in PBS buffer. HC<sub>50</sub> for each polymer is indicated by the line to the x-axis.



### Evidence for membrane disruption

The mechanism of action of the new polycations described here is expected to be similar to antimicrobial peptides and related synthetic polymers, relying on disruption of bacterial membrane integrity,<sup>16</sup> although that is almost certainly an overly simplistic view.<sup>17</sup> SEM images showed a transition from smooth to rough outer *E. coli* surfaces upon polycation treatment, and the appearance of blisters on treated *B. subtilis* cells (Figure S6).

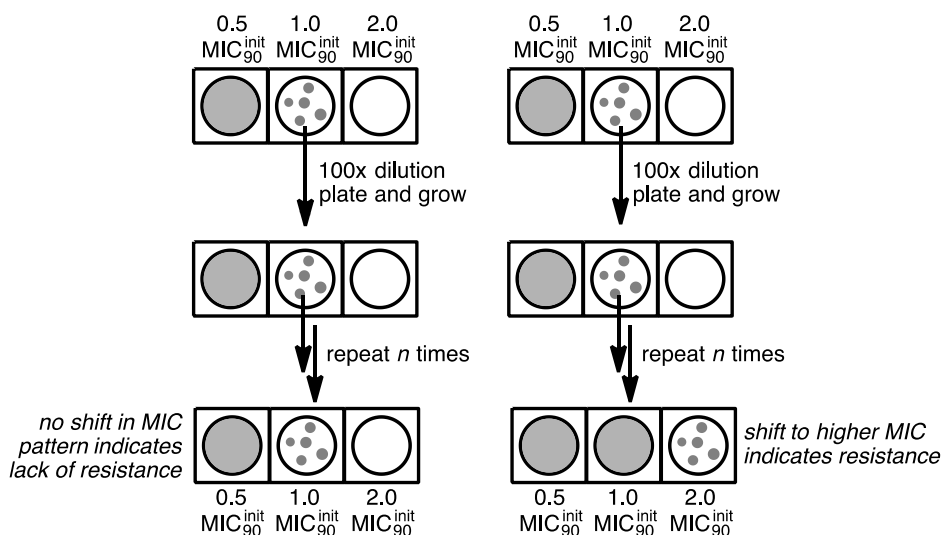
**Figure S6.** Morphology of bacteria before (A,C) and after (B,D) 1h treatment with polycation **3a** at 1  $\mu\text{g/mL}$ . *E. coli* is shown on the left (A,B) and *B. subtilis* on the right (C,D). Scale bars = 2  $\mu\text{m}$ .



### Measurements of antimicrobial resistance

Adapted from a standard assay method (Figure S7).<sup>18,19</sup> An *E. coli* culture grown in MHB media overnight was inoculated into wells of a 96 well microtiter plate containing MHB media and two-fold dilutions of the candidate antimicrobial around the previously determined  $\text{MIC}_{90}$  value (designated  $\text{MIC}_{90}^{\text{init}}$ ). These plates were incubated in gently rotating incubator-shaker at 37°C. Every 12 hours, bacterial growth was assayed by reading absorbance of the solution at 600 nm on a plate reader, and an aliquot of bacterial culture was removed from the well containing the highest concentration of antimicrobial agent allowing observable bacterial growth, defined as an absorbance value greater than above 0.015, with background absorbance at 0.01). Each aliquot was diluted 100 times in fresh MHB media and distributed into wells containing the same concentration range of antimicrobial agent (freshly prepared). When MIC towards certain antimicrobial shifted, the MIC of those evolved cells towards other antimicrobials was also evaluated.

**Figure S7.** Protocol for assessment of *E. coli* resistance to antimicrobial agents of interest. Dilution and re-plating was done twice a day.



Consistent with literature reports, we found the development of resistance to polycationic agents to emerge very slowly, as noted in the text and in Table S2. We do not yet understand the reason for the faster emergence of resistance towards the acyclic polyionene **5** compared to BCN polyionenes **3a** and **3m**. Note that after 60 passages, cells evolved against **5**, **3a** and **3m** also exhibited a doubling of MIC<sub>90</sub> against CPC without having been previously exposed to that agent.

**Table S2.** Number of passages before the doubling of MIC<sub>90</sub> was observed for each antimicrobial.

Antimicrobial	CPC	<b>5</b>	<b>3a</b>	<b>3m</b>
Number of passages before development of resistance	<28	33	54	60

### Surface modification and characterization

The ability to kill bacteria when adsorbed or attached to solid surfaces is useful in a number of contexts, including natural barrier membranes,<sup>20,21</sup> antimicrobial packaging,<sup>22,23</sup> and infection control in healthcare settings.<sup>24</sup> Cationic peptides and polymers are important in these efforts,<sup>25</sup> with a variety of examples showing dependence on charge density and other factors.<sup>26-28</sup>

Silicon wafers (1 cm x 1 cm), glass chips (1 cm x 1 cm), or glass beads (0.25 cm in radius) were cleaned with piranha solution for 30 min, sonicated with deionized water for 30 min, rinsed with methanol, and dried with N<sub>2</sub>. The cleaned substrate was immersed in a solution of 3-azidopropyl triethoxysilane (20 mM in toluene) overnight at room temperature. The substrate was then washed with methanol, dried under a N<sub>2</sub> stream and immersed in solution of polycation **3b** (1 mg/mL, 0.16 mM (3.2 mM in terms of monomer units), in 80/20 water/t-BuOH) with copper sulfate (5% equiv, 0.2 mM), sodium ascorbate (10% equiv, 0.4 mM) and THPTA ligand (5% equiv, 0.2 mM) overnight at room temperature in a closed vial. After washing with water and then methanol, the surface was incubated in a 1 mM aqueous solution of cysteine for 1 hour to remove adsorbed metal ions. After a final wash with methanol and drying under N<sub>2</sub>, the surfaces were characterized by XPS and contact angle measurements at at least three places with high

reproducibility between these values. Each substrate was cut into smaller pieces before use in antimicrobial assays.

*XPS results of glass surfaces after multiple rounds of antimicrobial testing and washing (Figure 3).* These results are shown in Table S3; note that the parameters measured here did not change significantly during these tests, while the antibacterial effectiveness of the surface reproducibly diminished in rounds 6-8.

**Table S3.** Characterization of glass surfaces after each round of microbial challenge.

# bacterial challenges / washes	C/Si	C/N	Contact angle
2 / 1	1.7	2.3	43
3 / 2	1.8	2.6	36
4 / 3	1.7	2.5	37
5 / 4	1.3	2.4	41
6 / 5	1.8	2.3	42
7 / 6	1.5	2.7	39
8 / 7	1.3	2.6	44
9 / 8	1.4	2.2	43

### **Antimicrobial control experiments for surface modified with covalently-attached 3b**

To ensure that the observed antimicrobial activity of polycation-functionalized glass was a function of the attached polymer, the cytotoxicity of various treated samples was assessed, summarized in Figure S8. The C/N ratios were measured by XPS for each sample prior to cysteine washing; toxicity against *E. coli* was assessed before and after the Cys wash.

Azide-modified glass samples exposed to CuAAC reaction conditions containing Cu<sup>+</sup> ions but no polycation (or the non-clickable **3a**) initially showed antibacterial activity, but not after washing with cysteine to remove adsorbed metal ions (panels 3A-3B, 5A-5B). The same result was observed with AgNO<sub>3</sub> (panels 7A-7B), tested because of the potential to import silver ions from the polymer synthesis procedure. Only CuAAC reaction with the clickable polycation **3b** gave rise to robust antibacterial activity after washing with cysteine (panels 2A-2B). The CuAAC attachment of small-molecule cation **6** (confirmed by a modest increase in observed C/N ratio) gave rise to only a small increase in antibacterial function.

Condition	Active cpd	before Cys	C/N	after Cys
Water	None			1B
Cu <sup>+</sup> , ligand	<b>3b</b>	2A	5.3	2B
Cu <sup>+</sup> , ligand	None	3A	2.5	3B
none	<b>3b</b>		3	4B
Cu <sup>+</sup> , ligand	<b>3a</b>	5A	4.4	1B
Cu <sup>+</sup> , ligand	<b>6</b>		3.6	6B
AgNO <sub>3</sub>	None	7A	2.1	7B
AgCl	None		2.2	8B

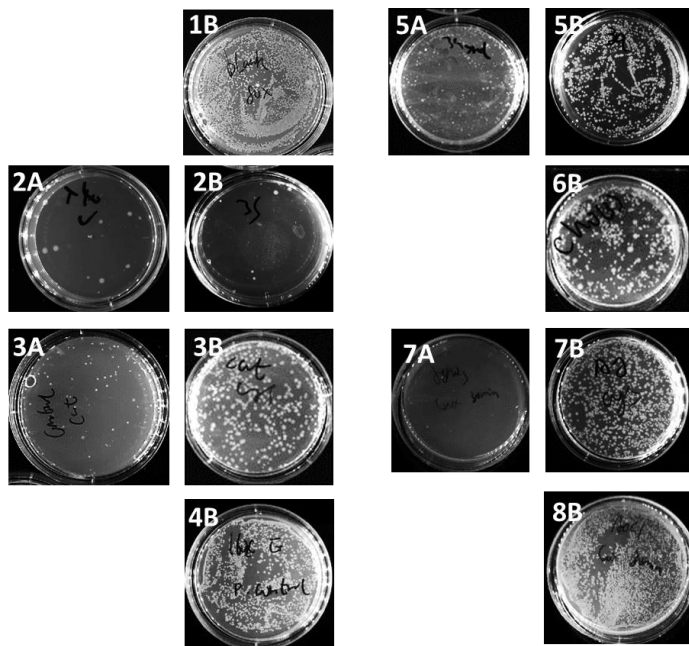
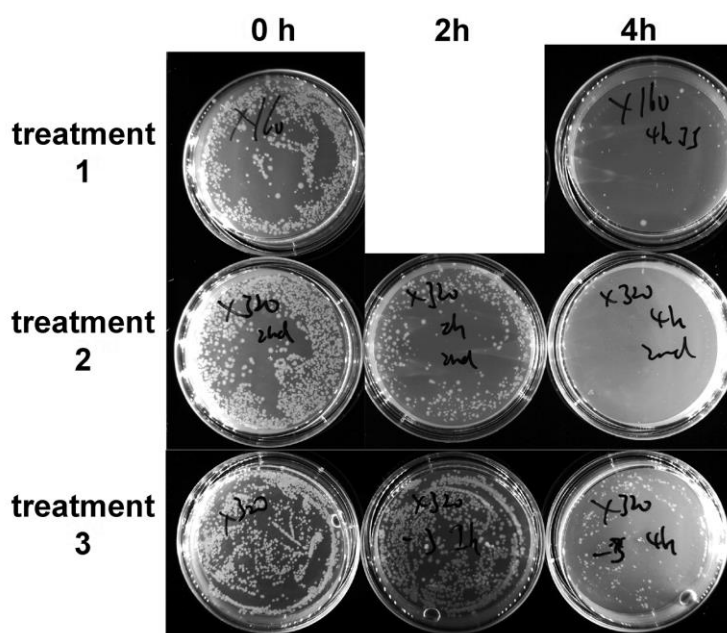


**Figure S8.** Control experiments with different surface treatment conditions and their respective antimicrobial activity before and after standard cleaning protocol. “Before Cys” and “after Cys” refer to the incubation of the glass chip in a 1 mM solution of cysteine in buffer with sonication for 3 minutes in a standard benchtop glass-cleaning sonicating bath; the entries in these columns refer to the images at the right.

### Repeat antimicrobial activity without washing

A glass chip covalently modified with **3b** was used repeatedly as in Figure 4 but without the sonication cleaning step between each cycle. The results of agar plate culture of the mixtures resulting from chip incubation for 0, 2, and 4 hours are shown in Figure S9. The antimicrobial efficiency increased with longer incubation in the presence of the chip. The approximate limit of killing efficiency at the third cycle was  $4 \times 10^6$  cells per/mL.

**Figure S9.** Viability of cells after being treated with single polymer coated glass chip at low initial concentration of *E. coli* ( $4 \times 10^4$  cells). The chip was repeatedly used without washing. Aliquots of the cell suspension were taken at the start (0 hours) and after 2 and 4 hours of incubation.



### Harsher washing conditions for reuse of derivatized glass

In addition to flat glass slides, glass beads were derivatized with polymer **3b** to test antimicrobial activity. After one use in the antimicrobial assay by **method B** (with similar results as the glass slide), the beads were sonicated in PBS for 20 min, water for 20 min, acetone for 1 hour, and finally with water again for 20 min, comprising a washing cycle of 2 hours. This cycle of testing and washing was repeated a total of four times, with results shown in Figure S10.

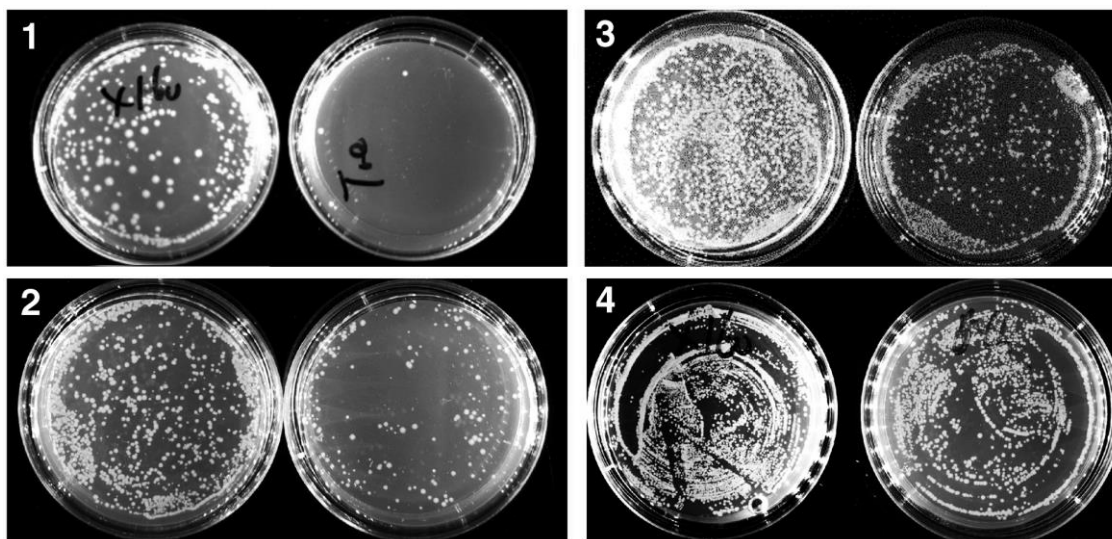
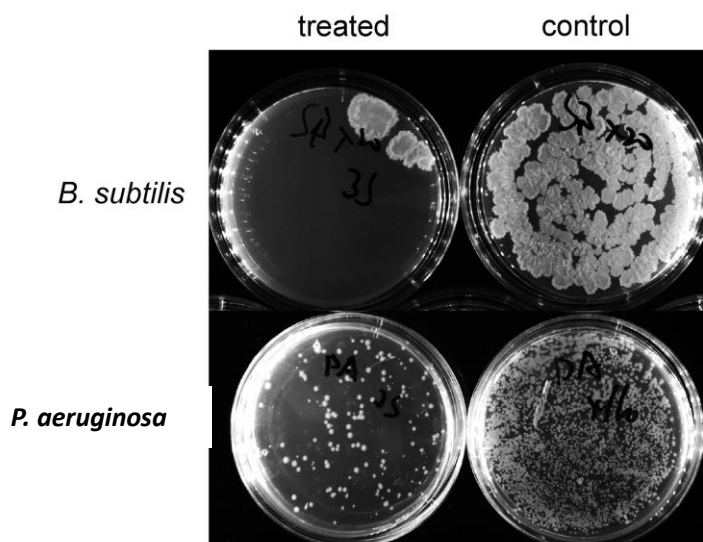


**Figure S10.** Antimicrobial activity in PBS buffer against *E. coli* of glass beads derivatized with **3b** and washed with the harsher two-hour protocol described in the text above. Each number refers to the wash cycle. Note that the last (4<sup>th</sup>) cycle was done with 1% Triton X-100.

### Antimicrobial activity towards *B. subtilis* and *P. aeruginosa*

Separate suspensions of *B. subtilis* ( $6.4 \times 10^5$  cells) and *P. aeruginosa* (PAO1-GFP) ( $8 \times 10^4$  cells) were treated with glass chips ( $0.01 \text{ cm}^2$ ) that had either not been treated (“control”) or covalently derivatized with **3b** as above (“treated”) for 4 hours in PBS buffer. Aliquots were then used to inoculate agar plates as described above in **Method B**. Representative plates after 24 h incubation are shown in Figure S11.

**Figure S11.** Demonstration of antibacterial activity against *B. subtilis* (top) and *P. aeruginosa* (bottom) of a glass surface bearing polycation **3b**.



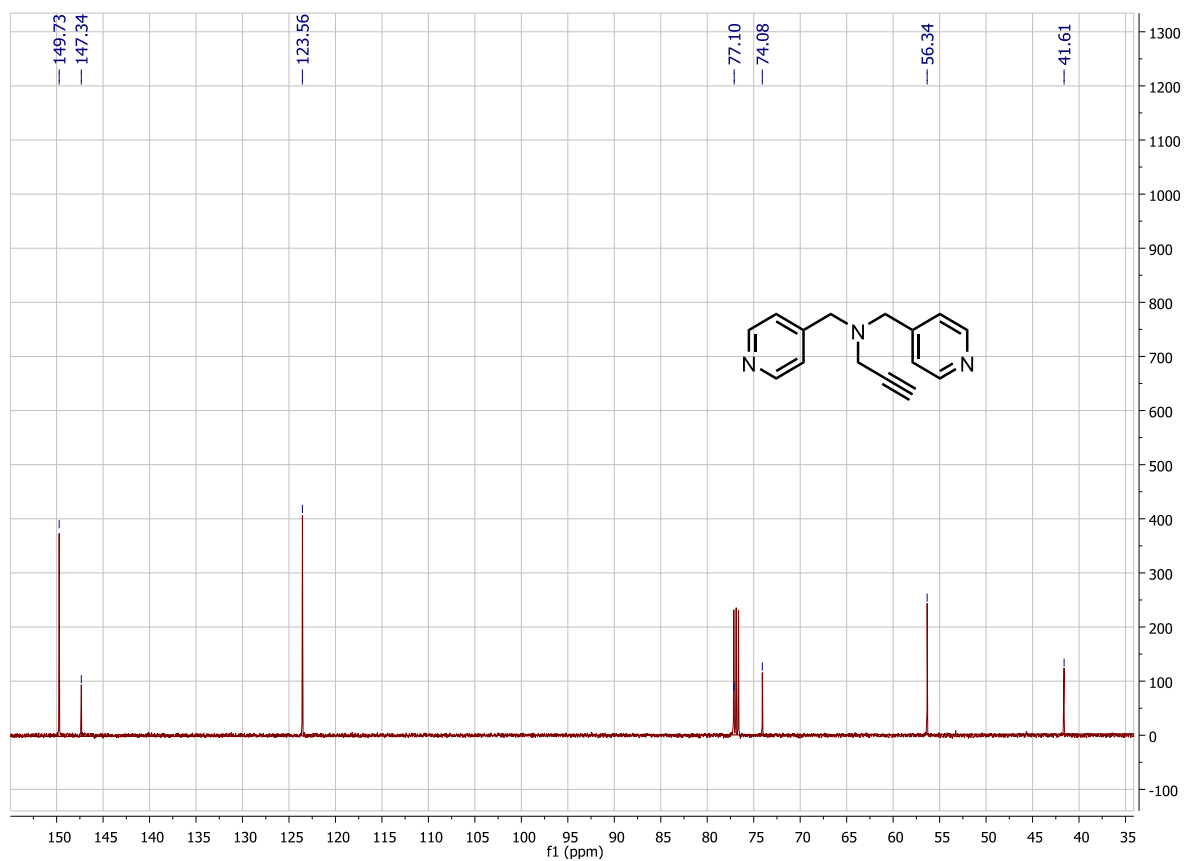
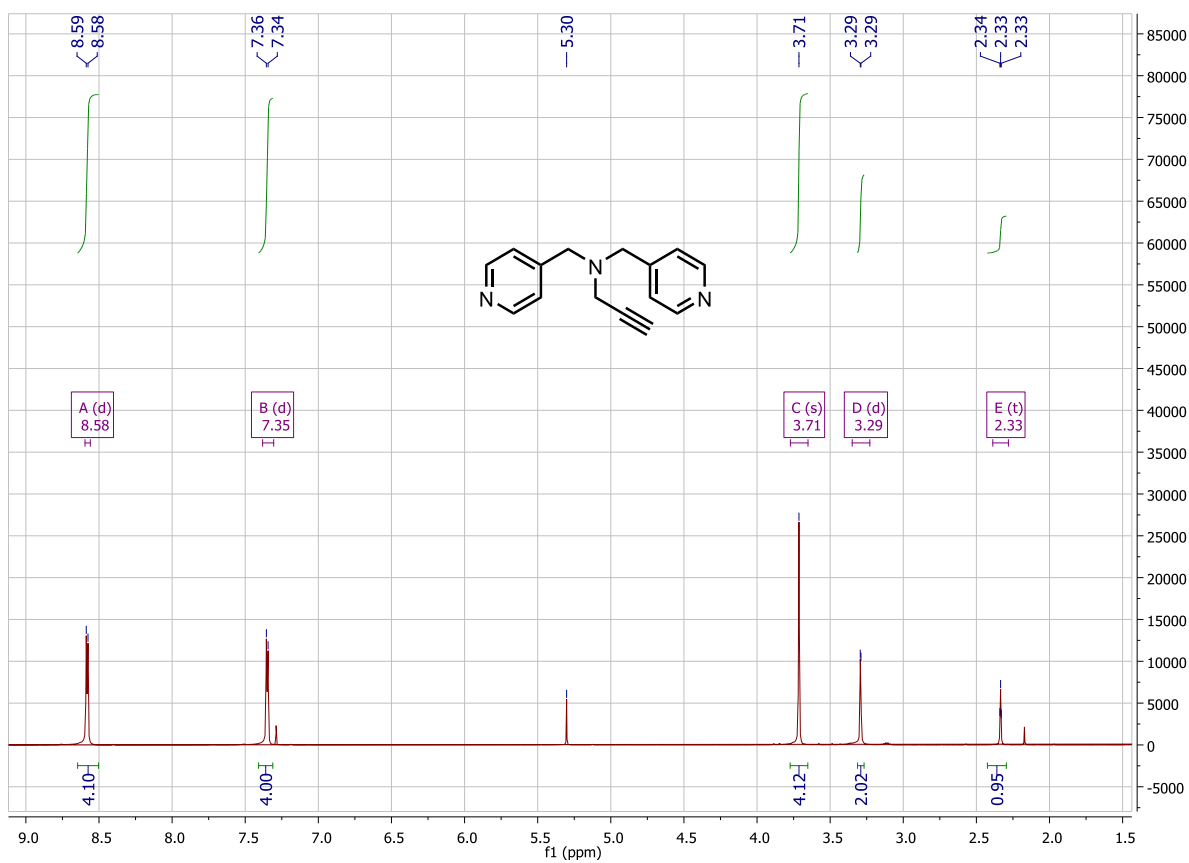
### Mammalian cell viability in contact with derivatized glass chips

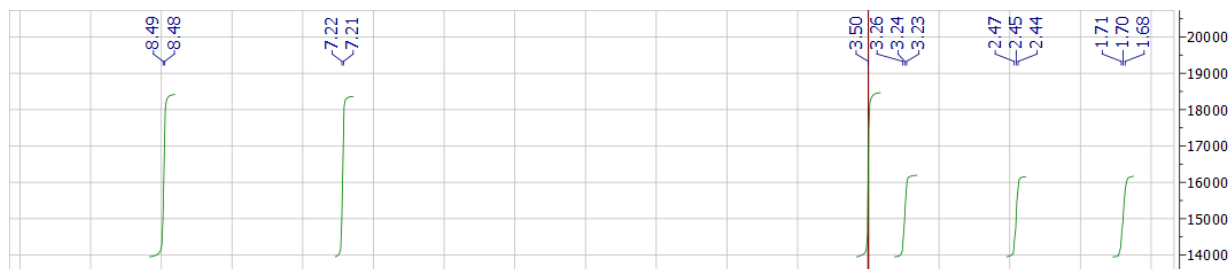
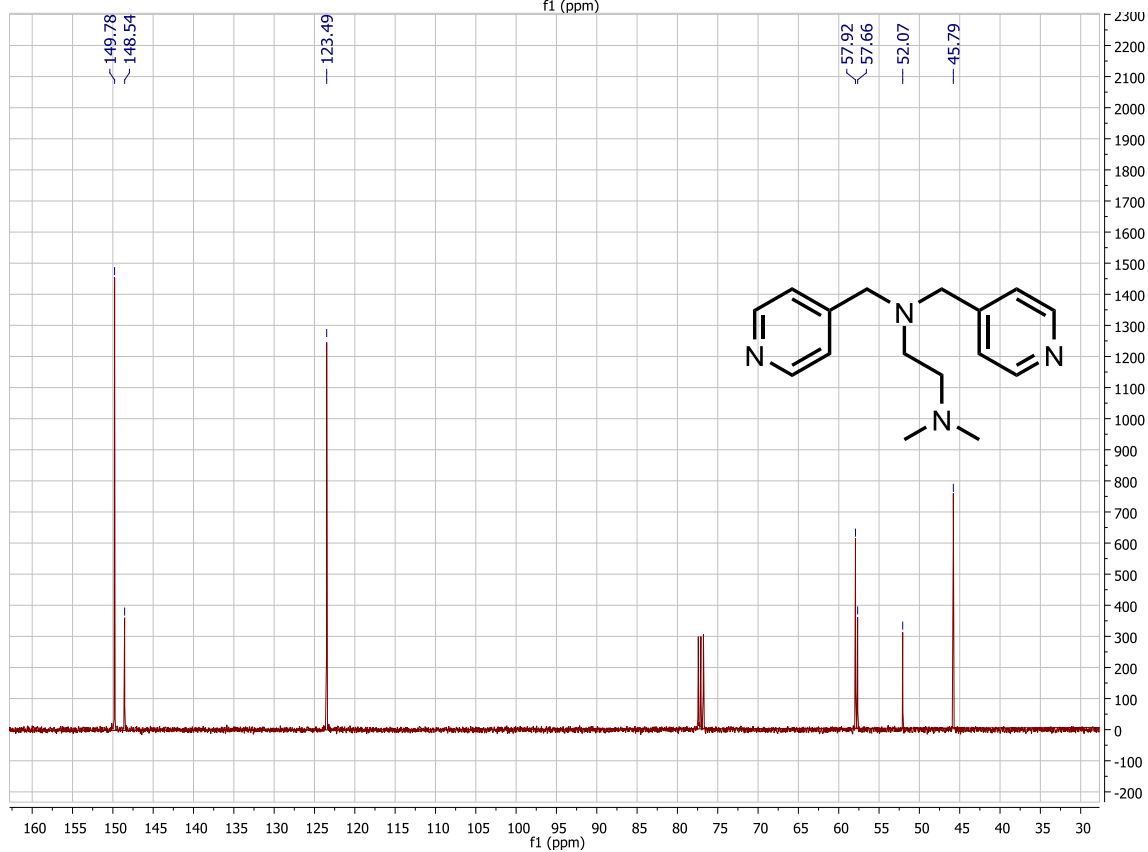
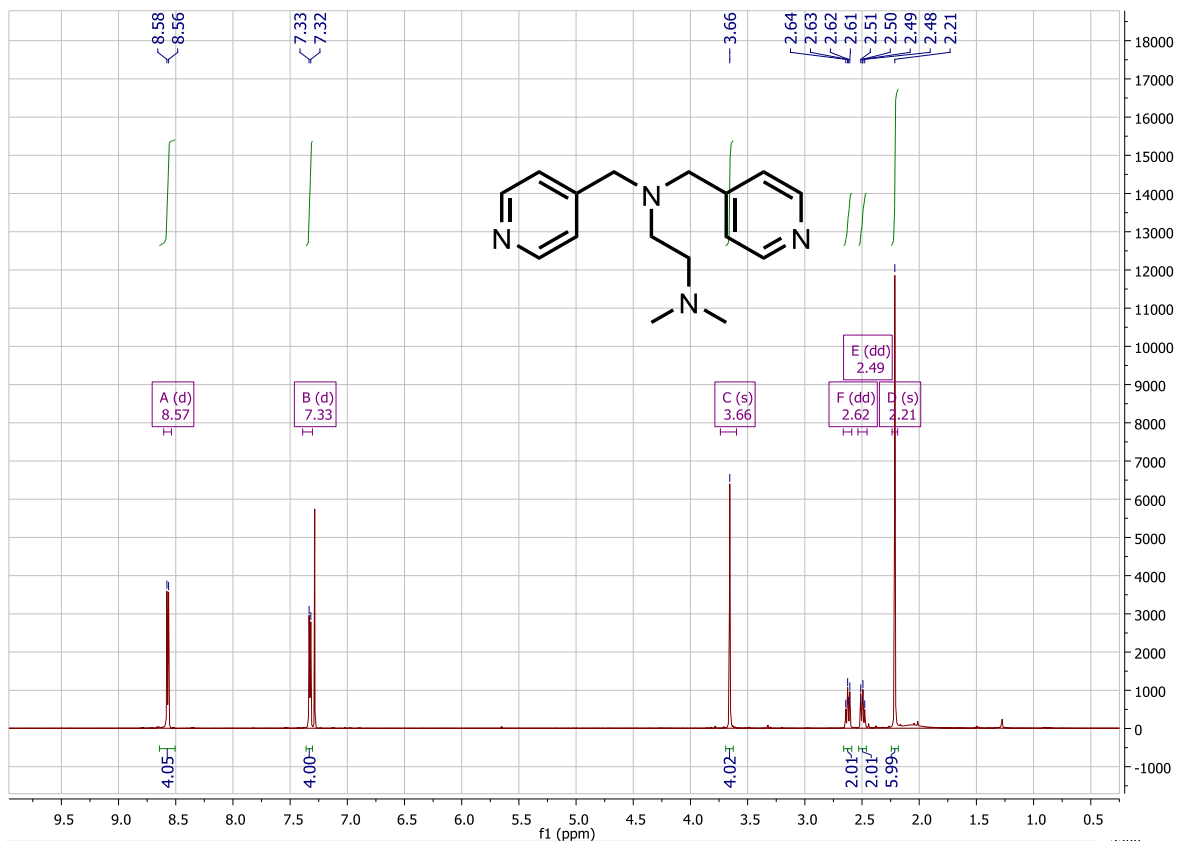
Jurka cells (approximately  $1 \times 10^5$  per well) were plated in a 96-well plate in 100  $\mu\text{L}$  of complete growth media or PBS buffer at 37 °C. A glass chip coated with BCN polycation **3b** (approx..  $0.01 \text{ cm}^2$  in area) was immersed in the cell suspension. After 4 or 24 h, cell viability was measured by MTT assay, with non-treated cells assigned as 100%. No cytotoxicity was observed, with both 4- and 24-hour incubations returning results showing  $100 \pm 5\%$  viability.

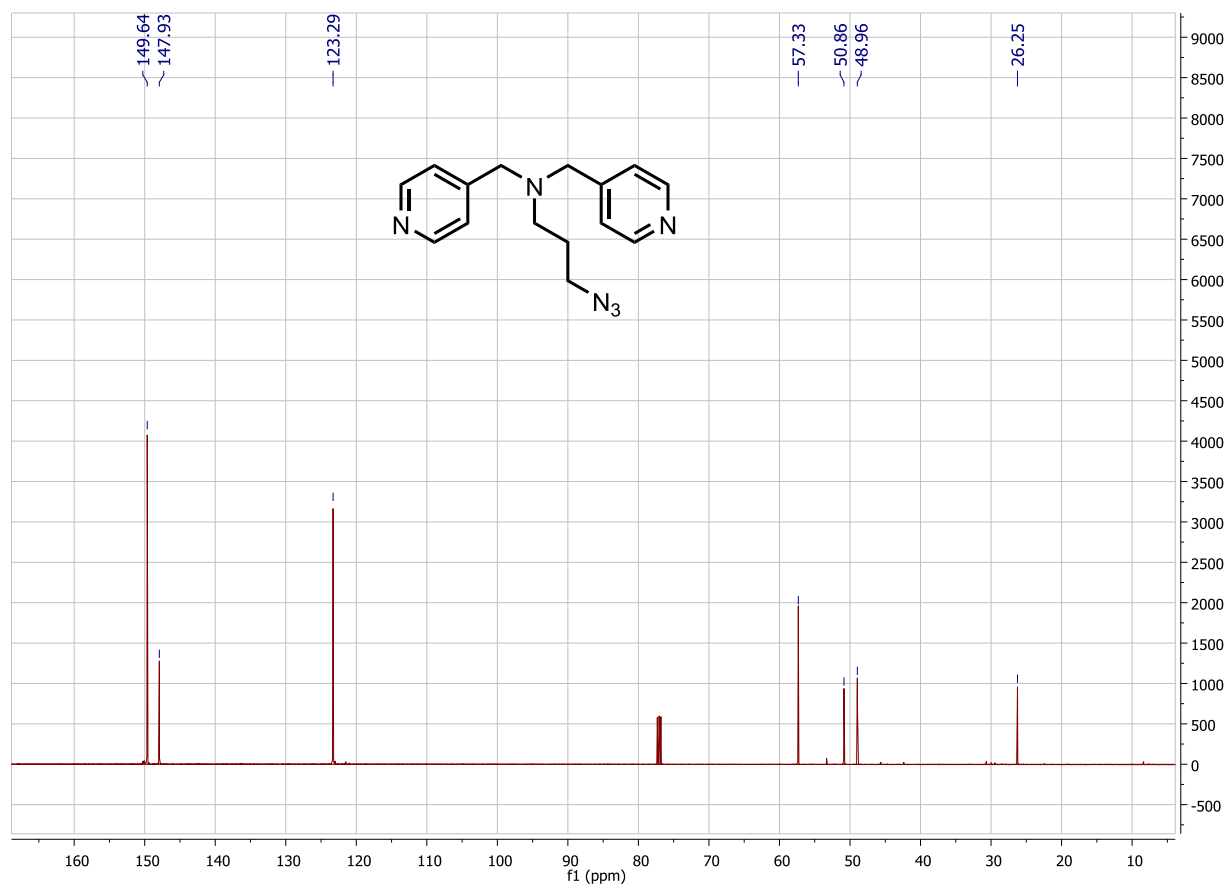
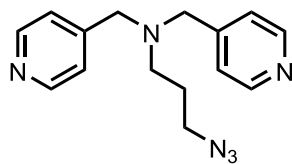
### Scanning electron microscopy (SEM) measurements

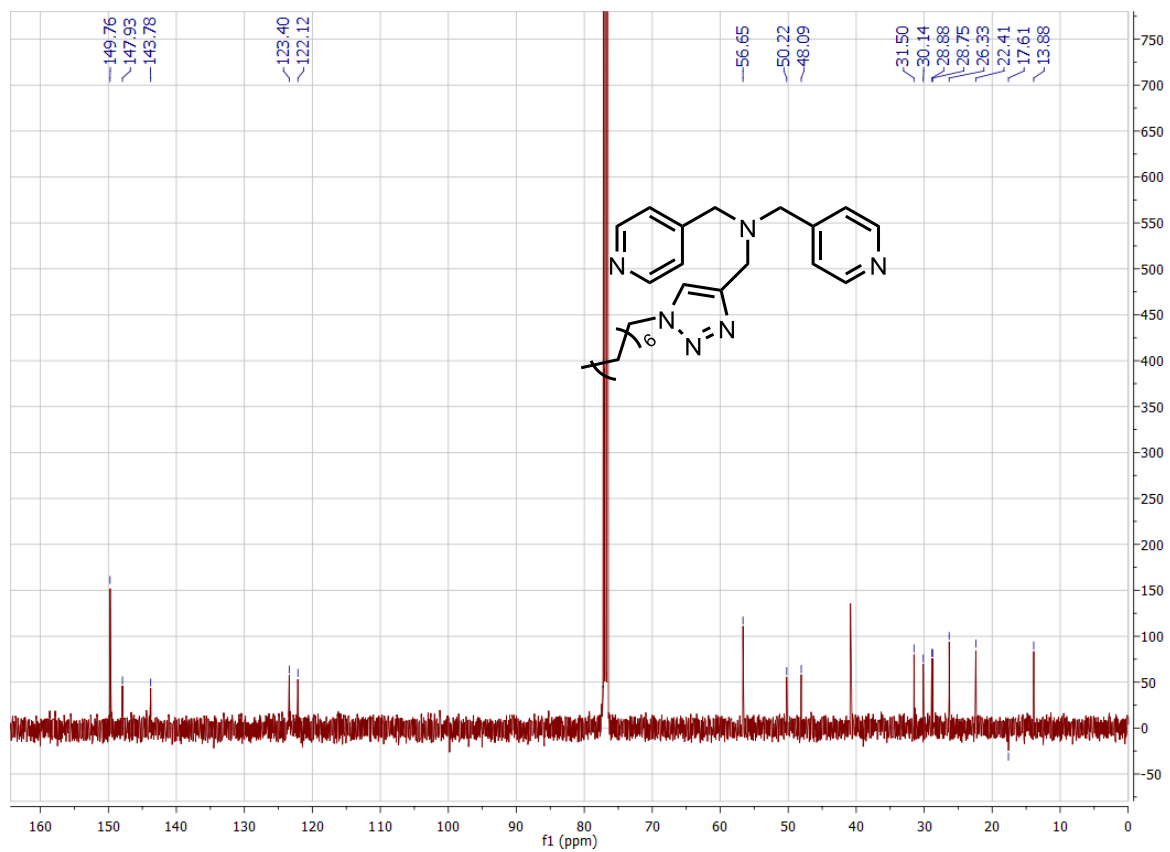
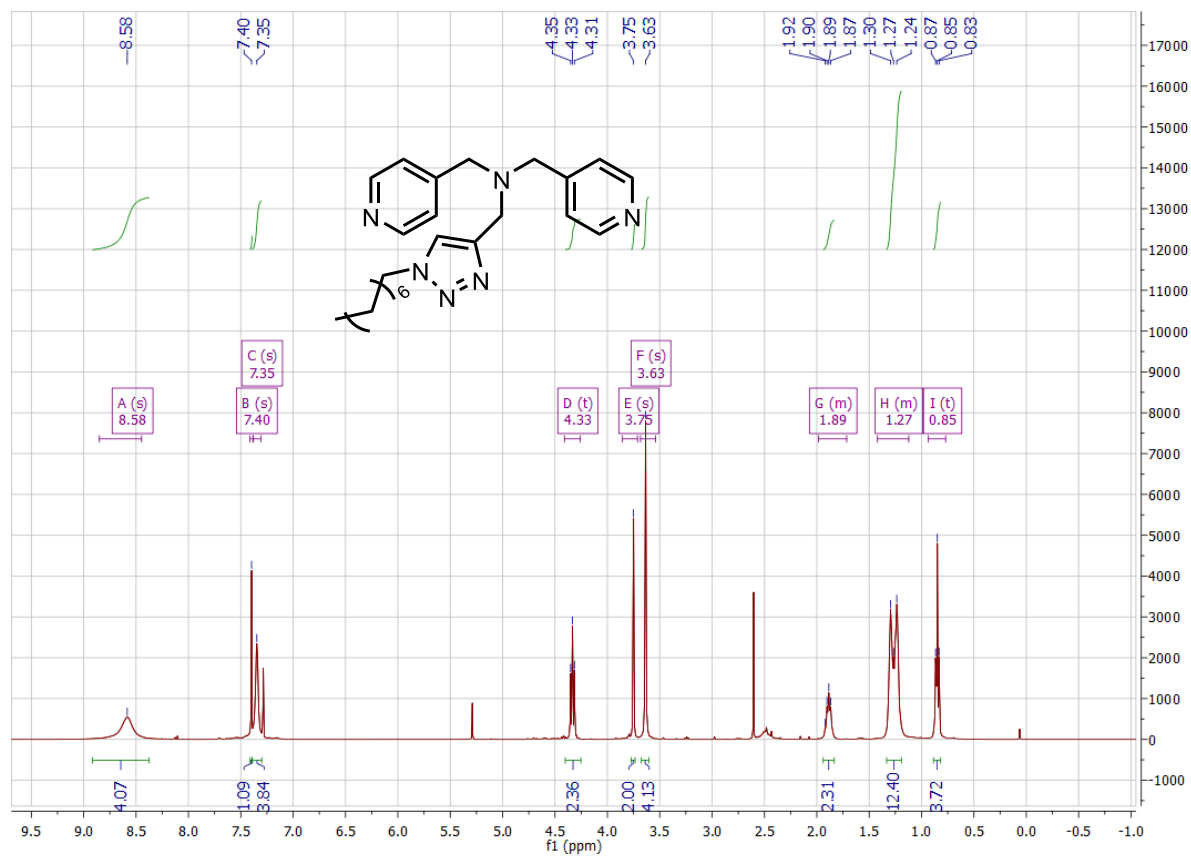
After treatment with the antimicrobial agent of interest, bacteria were immediately fixed with glutaraldehyde (0.5%) in PBS at room temperature for 30 min. The bacteria were centrifuged (3500 g for 10 min) and the supernatant was removed, and the resulting pellet was suspended in sterile water. A 1  $\mu\text{L}$  aliquot of the bacterial suspension was added to a clean piece of mica and allowed to dry in air. Immediately after drying, 0.1% glutaraldehyde was added for further fixation for 2 h. The resulting the specimen was washed with sterile water and dehydrated by addition of ethanol in a graded series (70% for 5 min, 90% for 5 min, and 100% for 5 min) and then dried in air. Finally, each specimen was sputtered with gold before examination with SEM (SU8230, Hitachi).

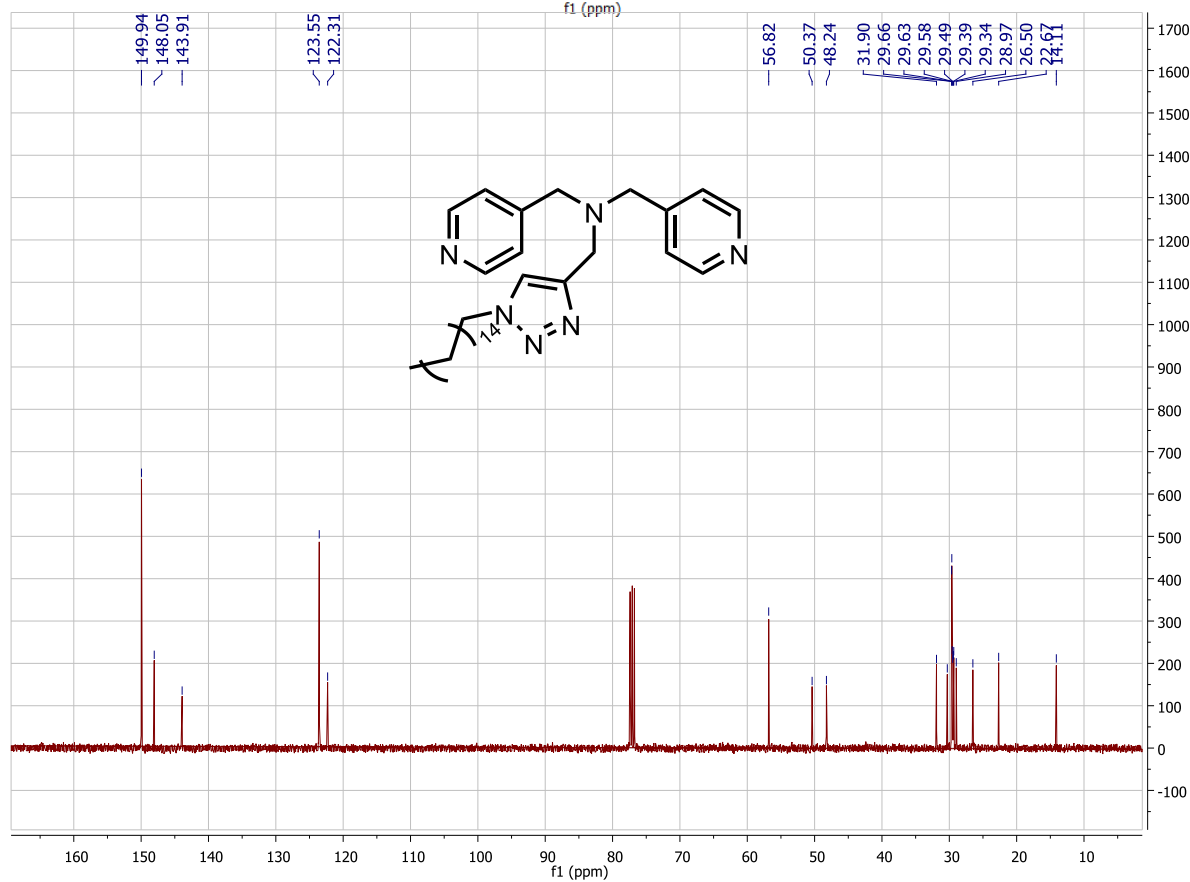
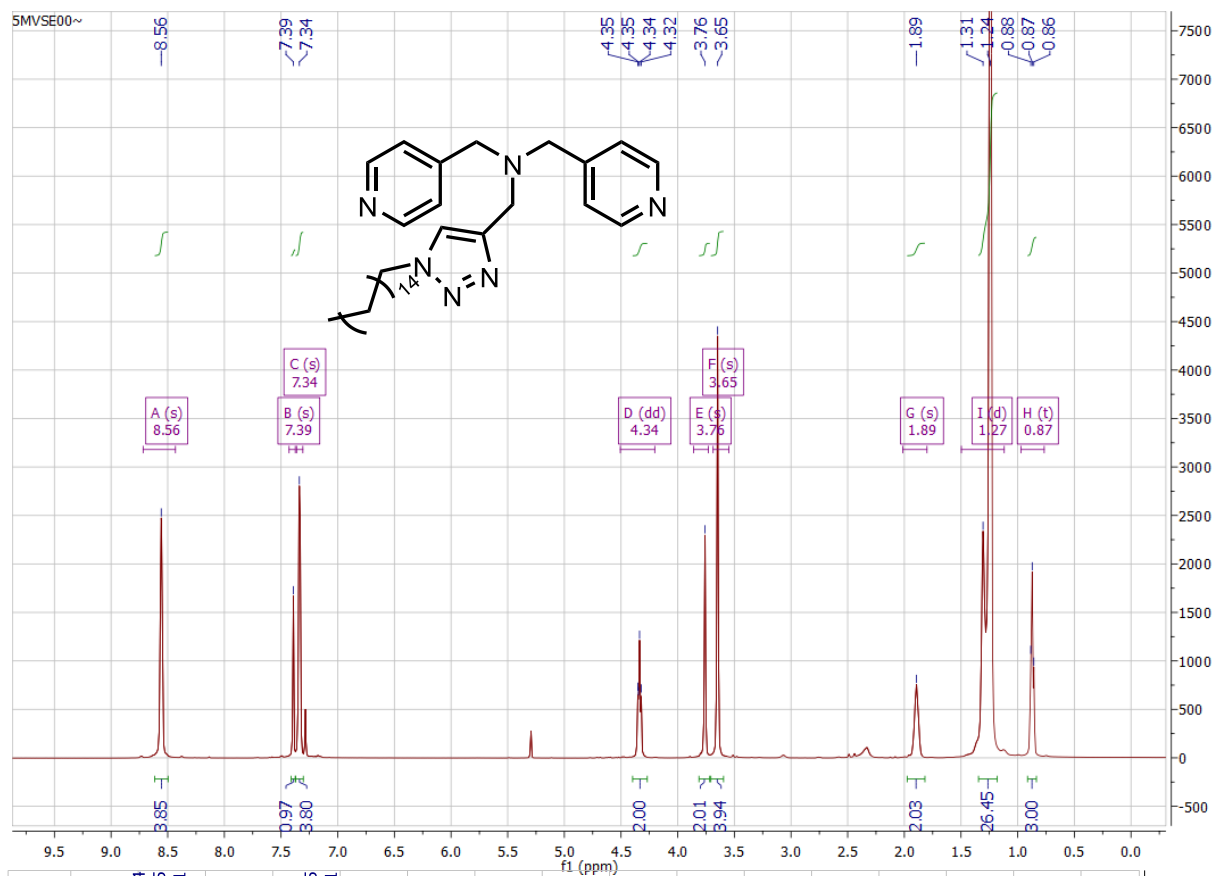


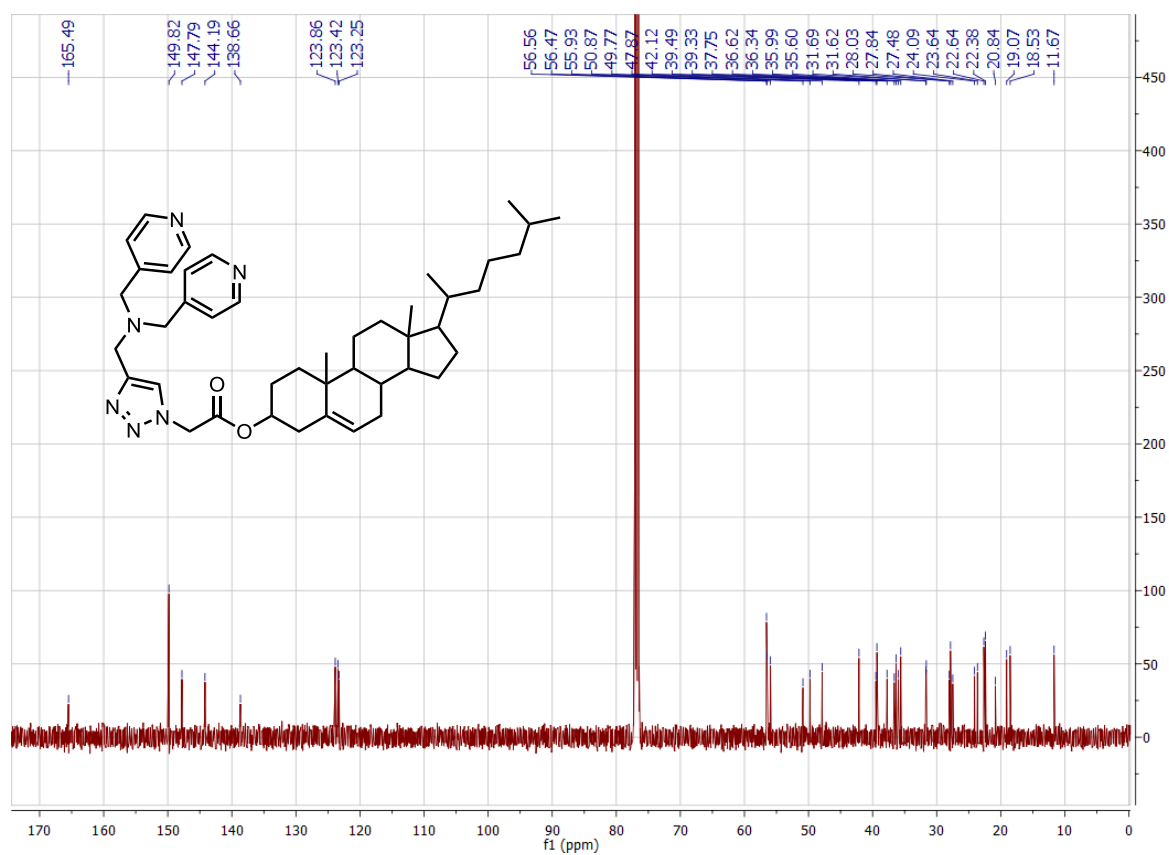
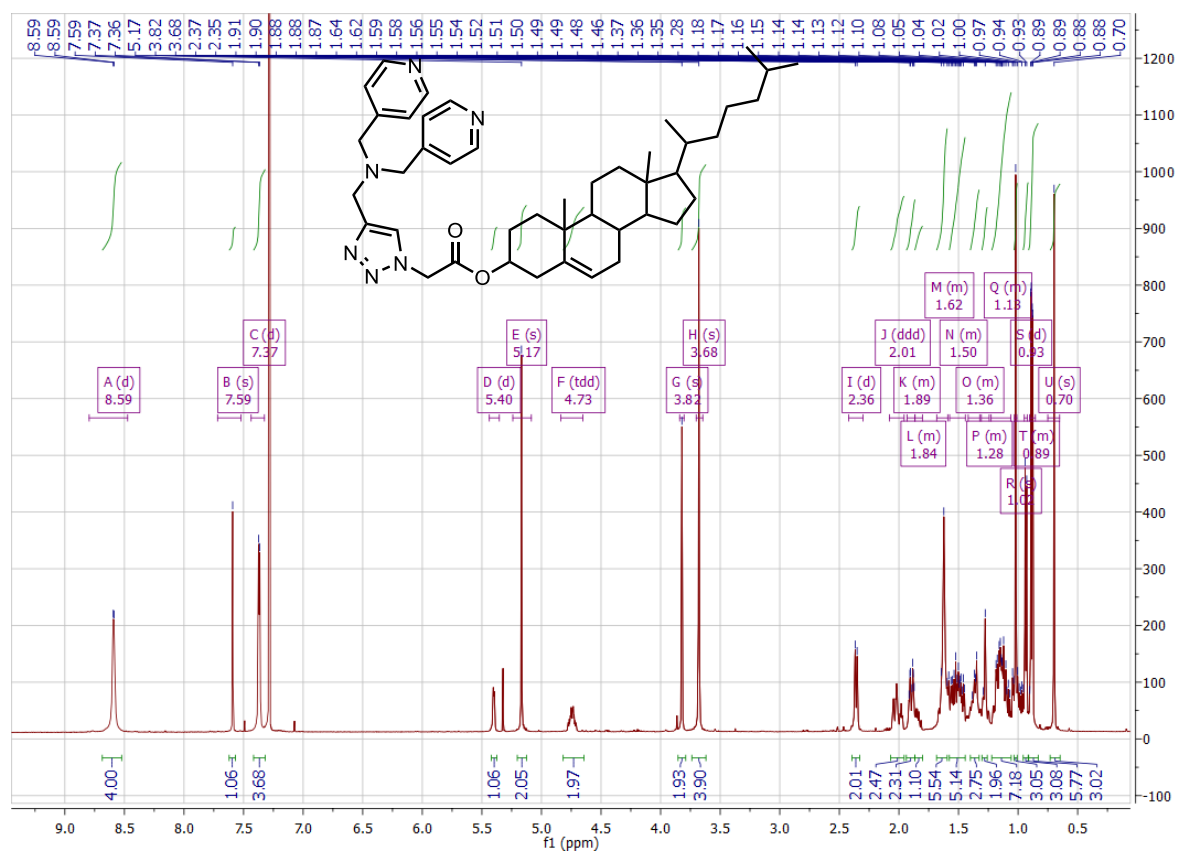


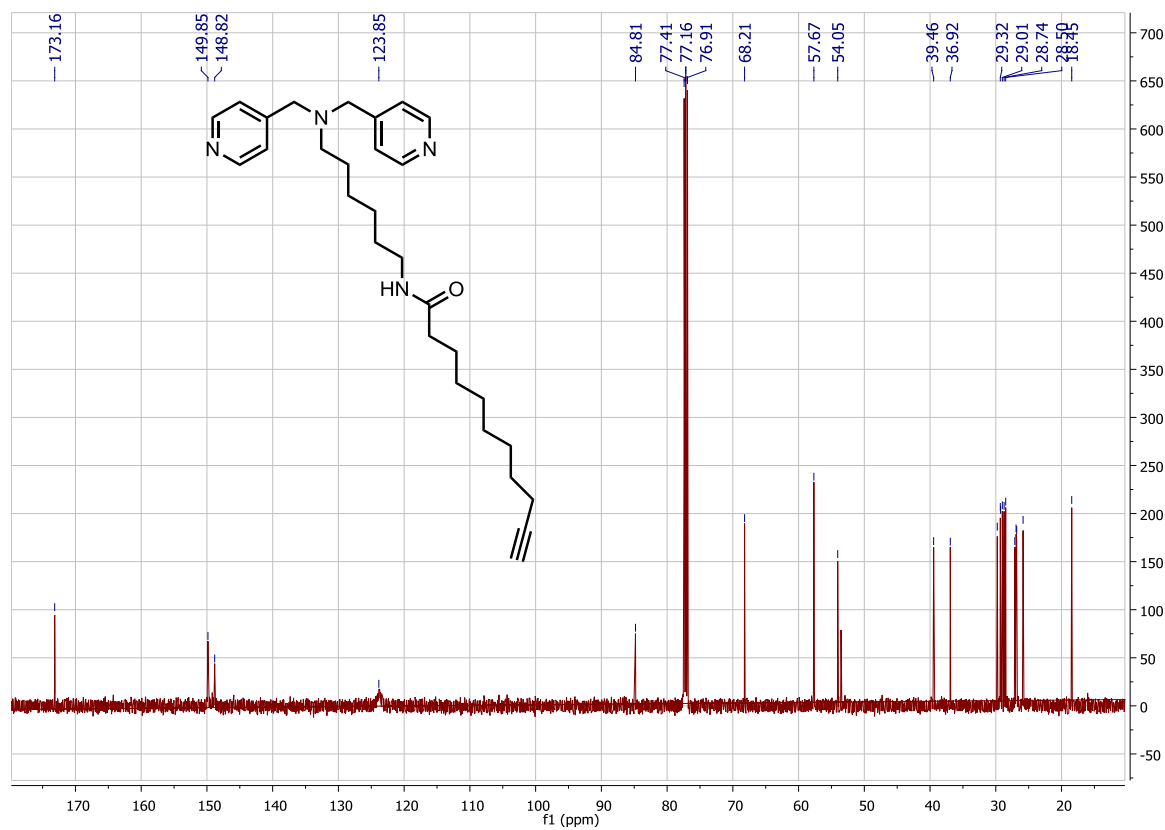
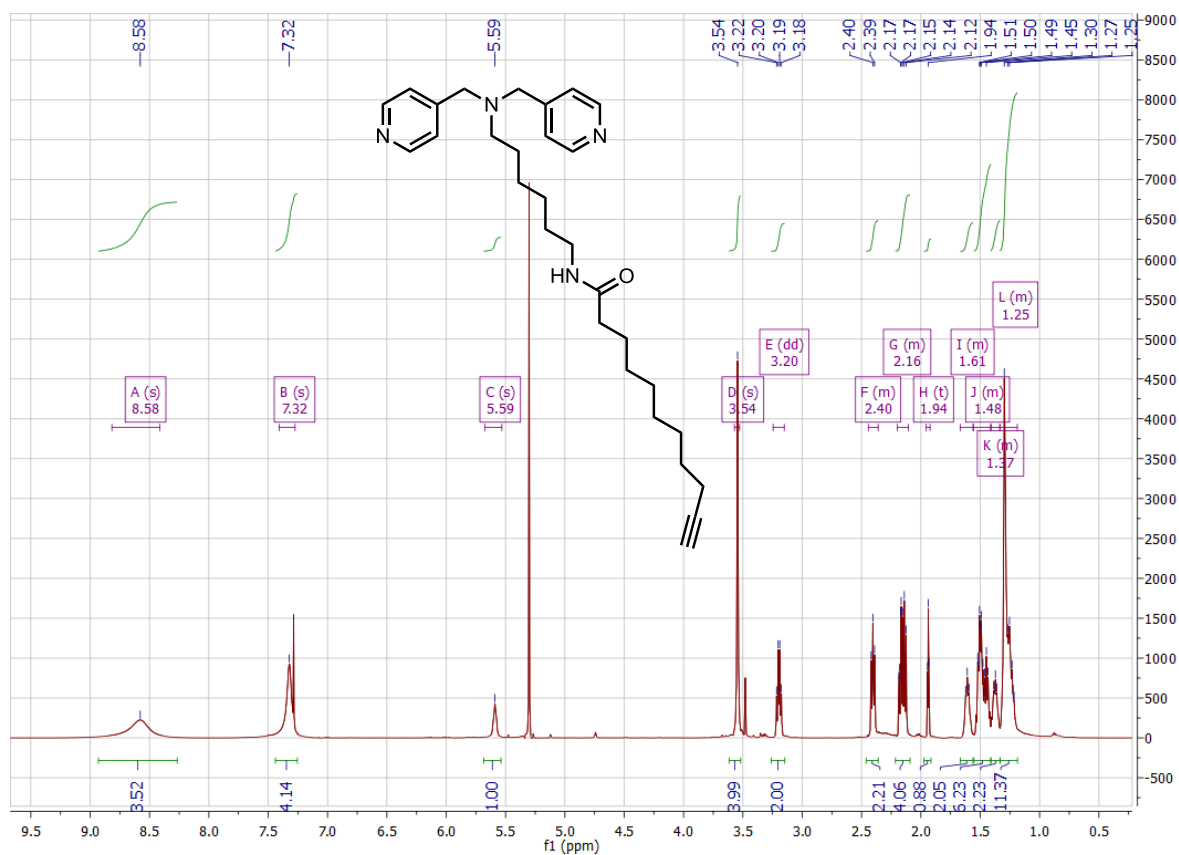


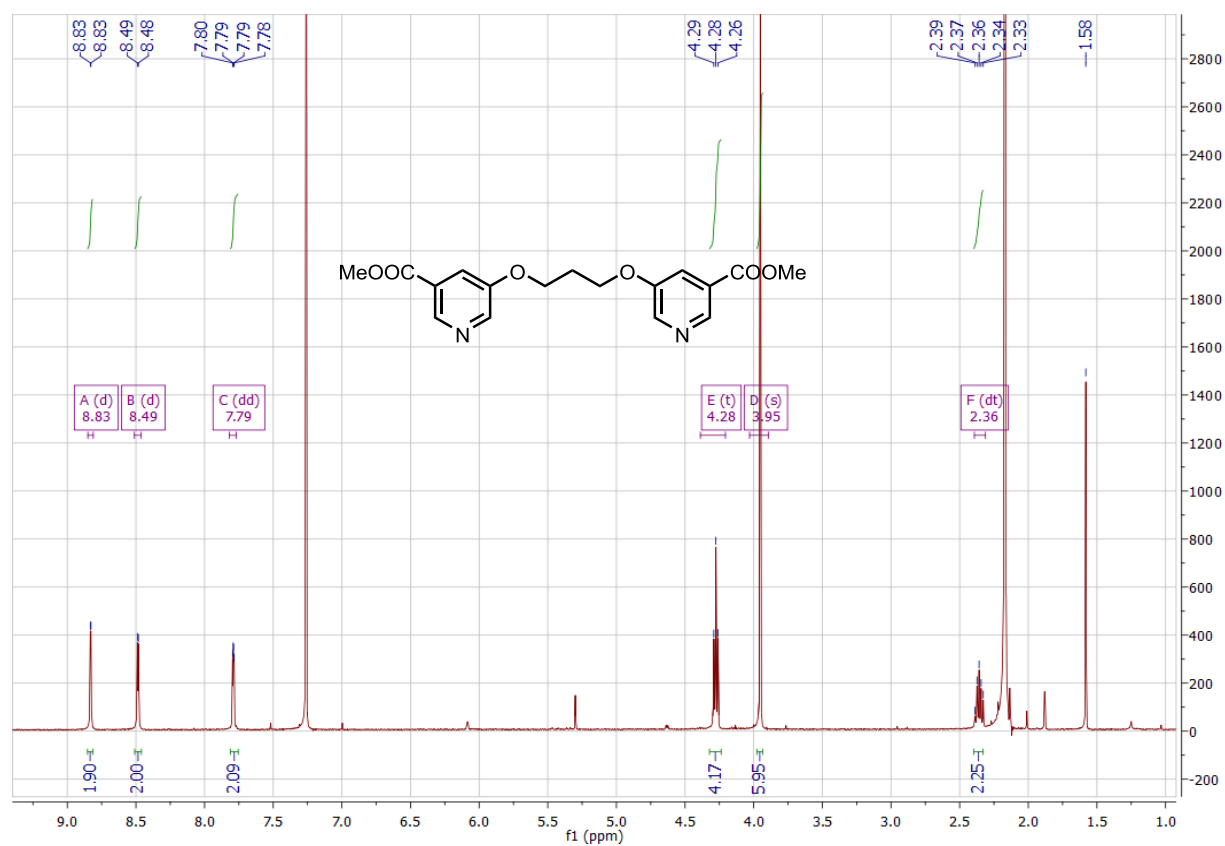




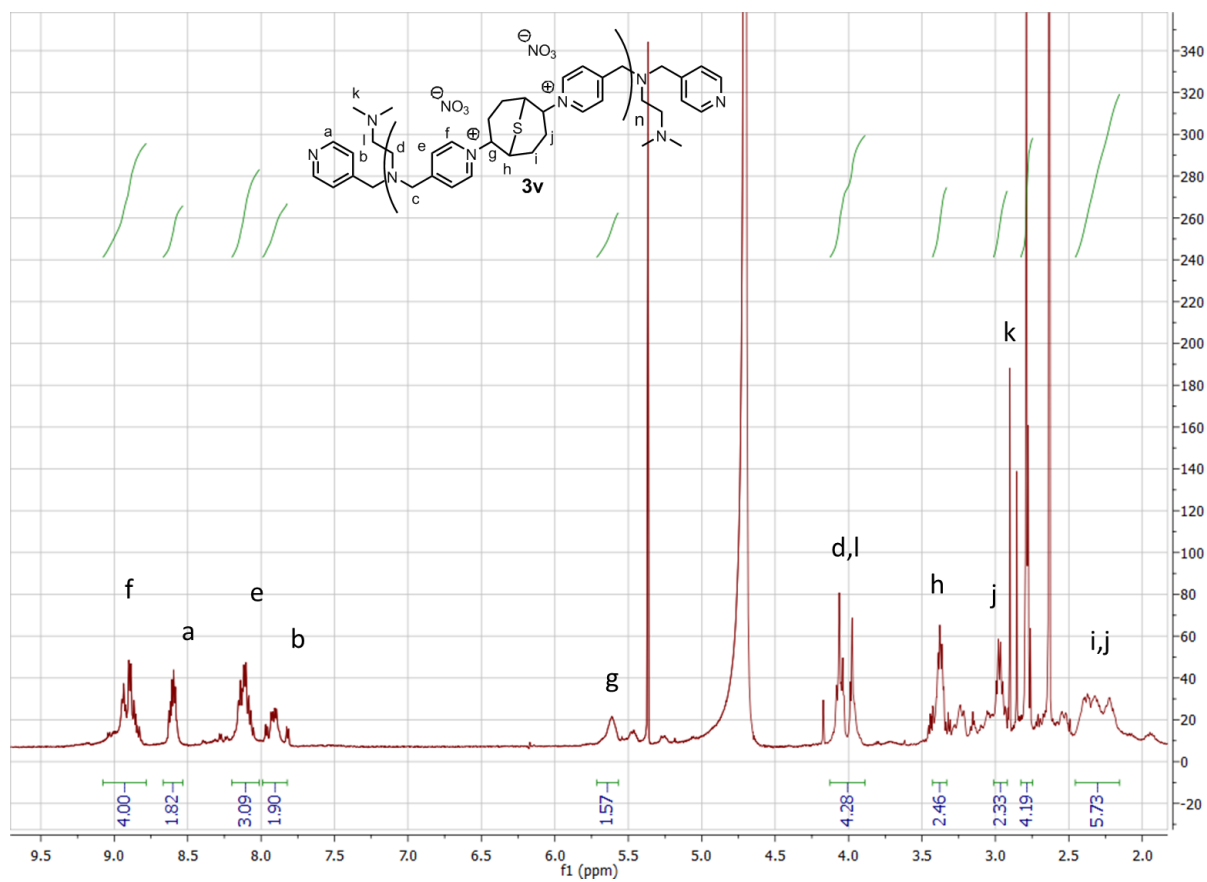
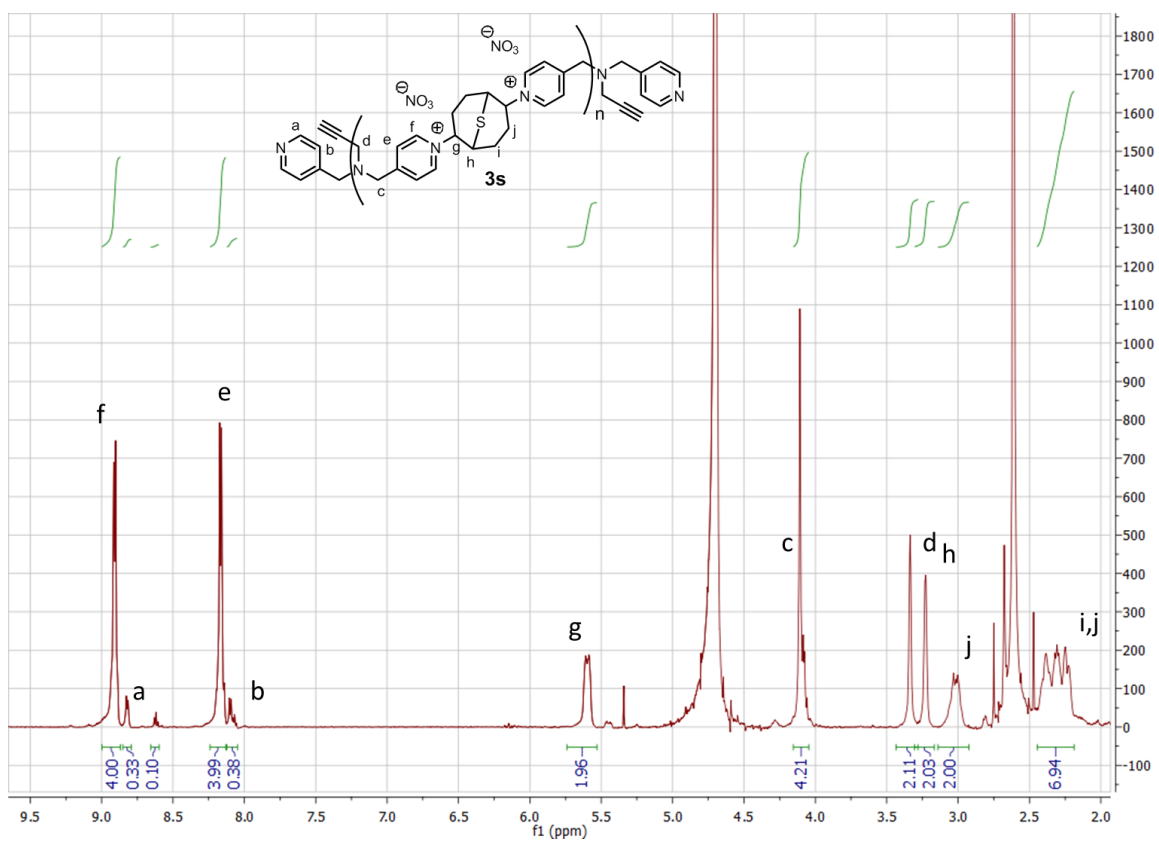


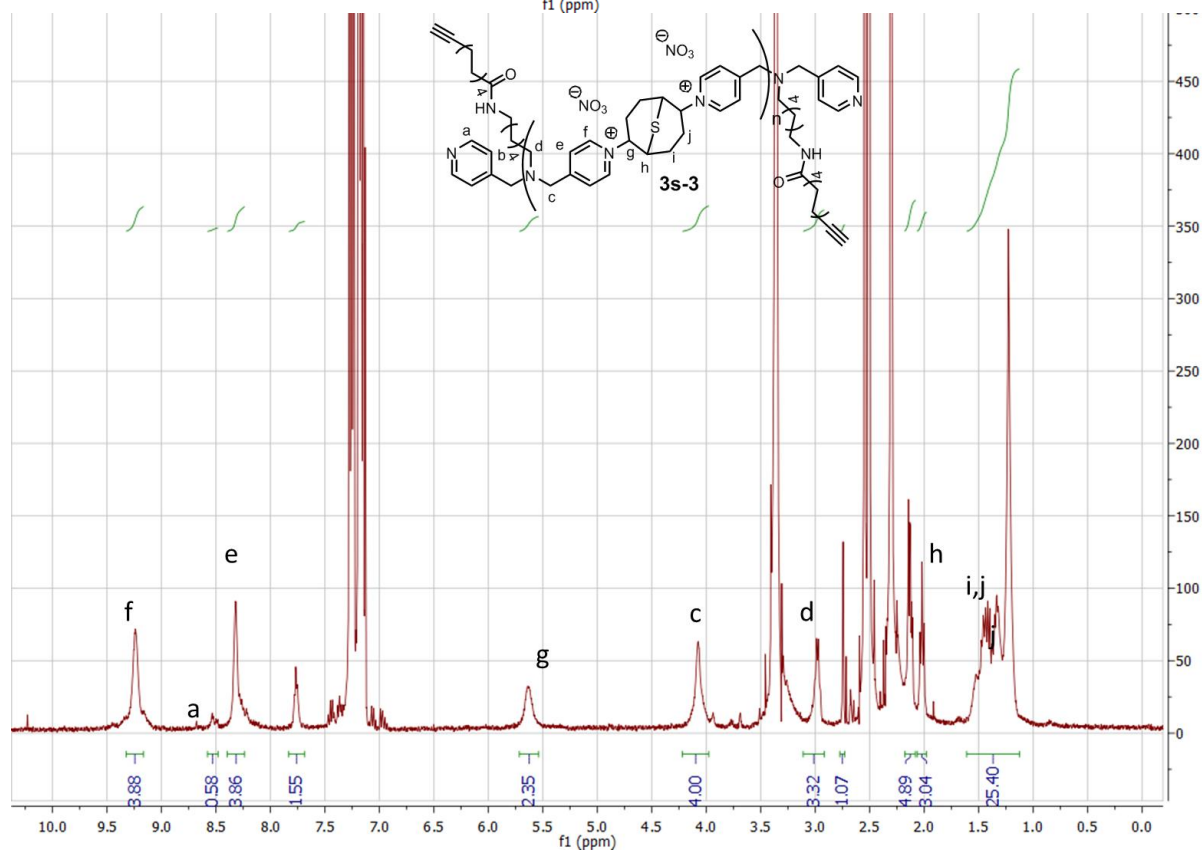
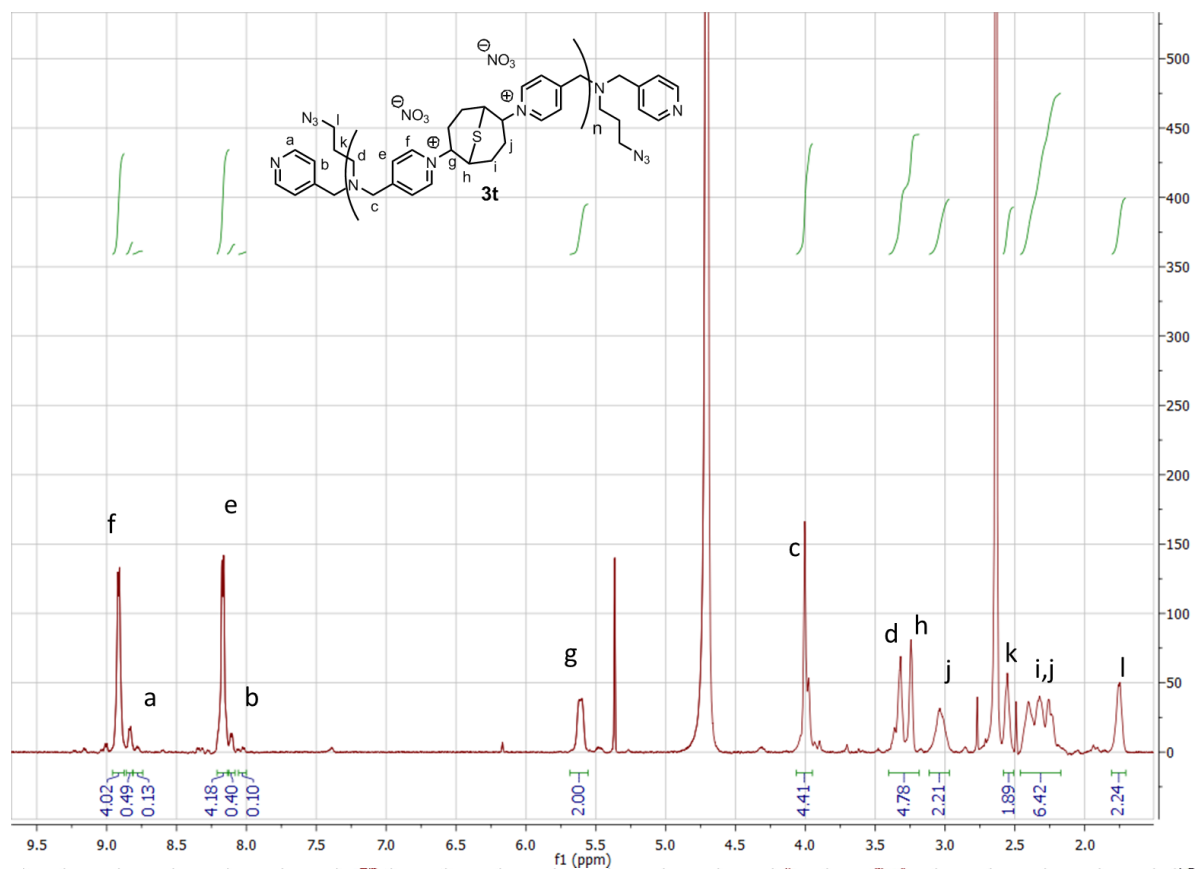


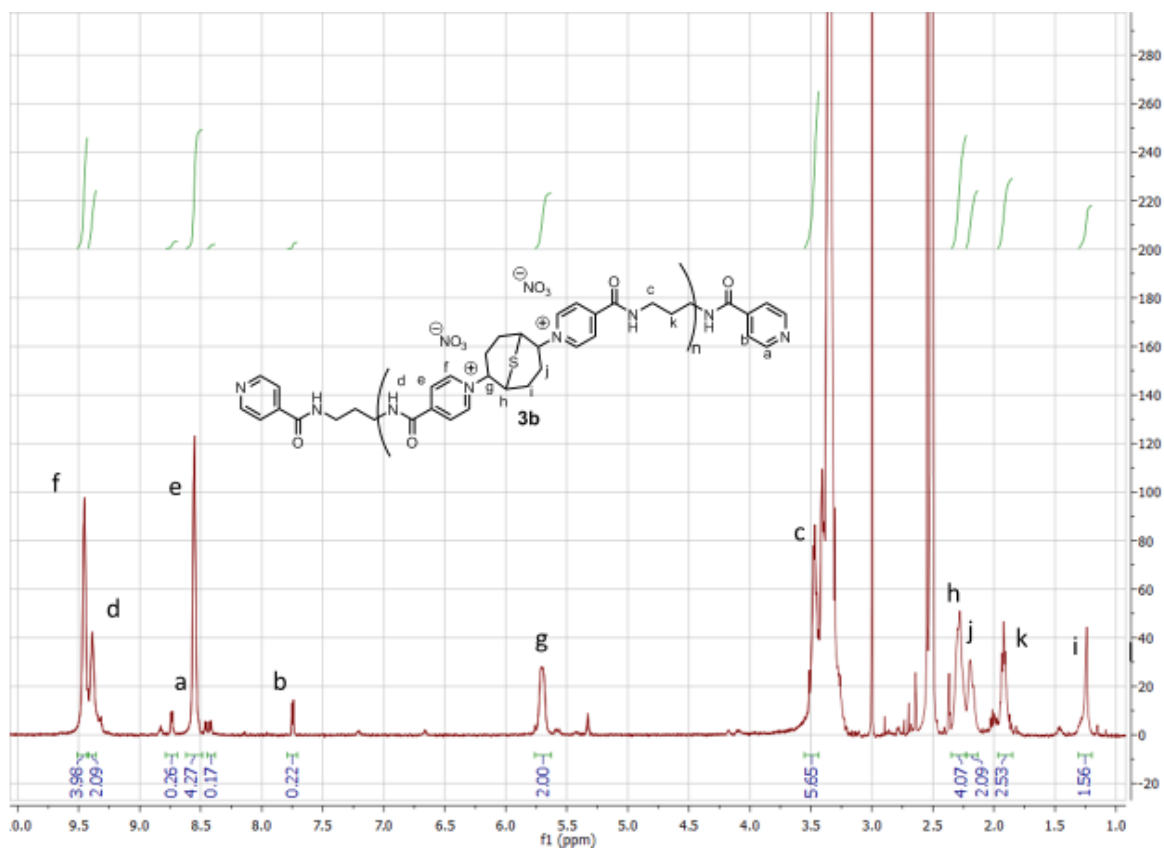
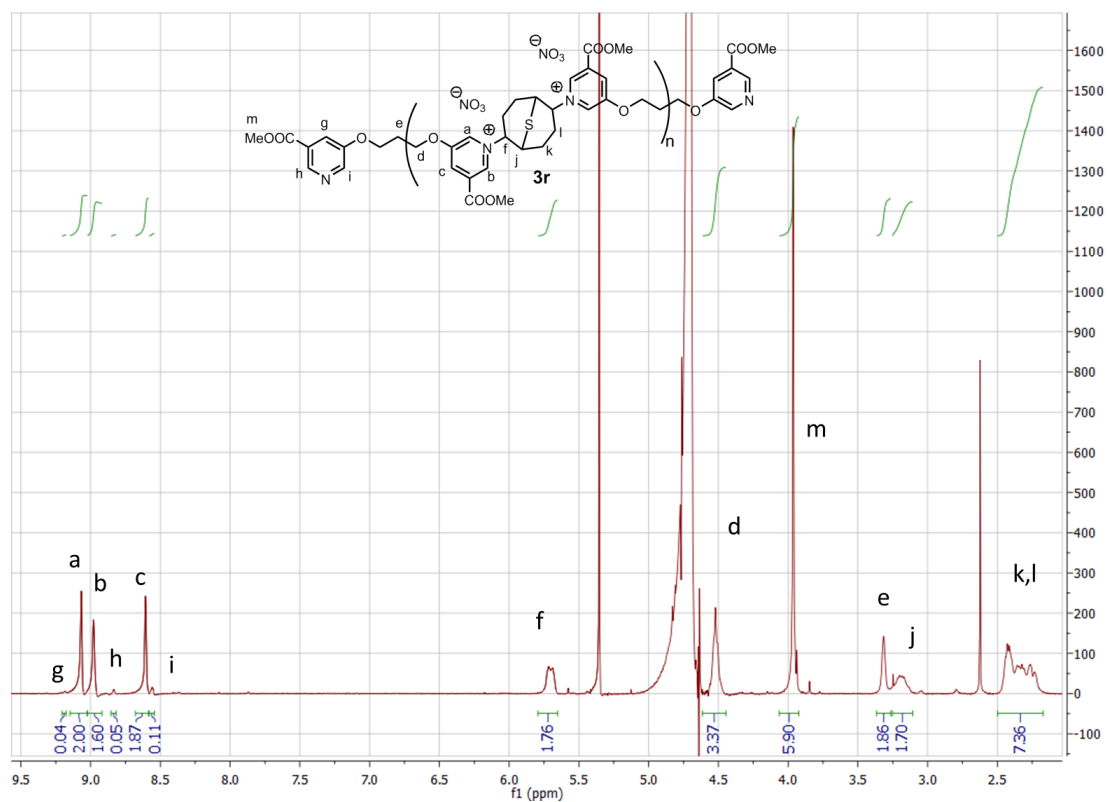


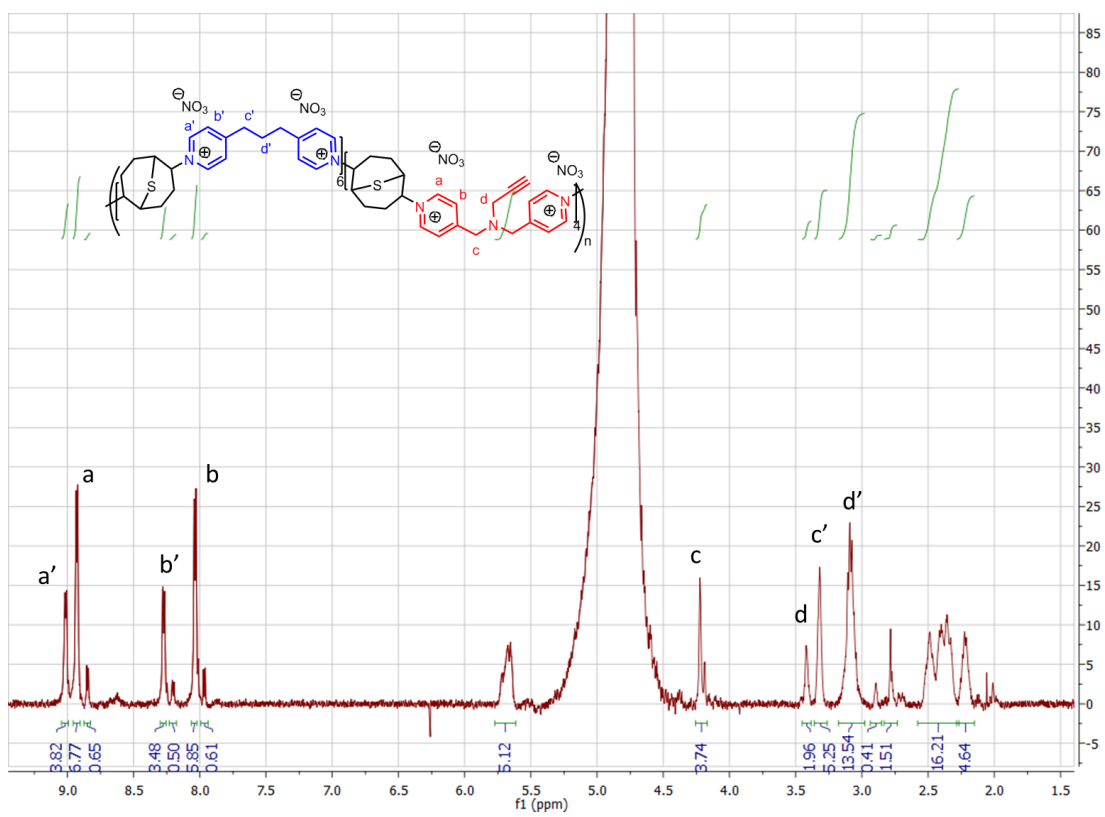


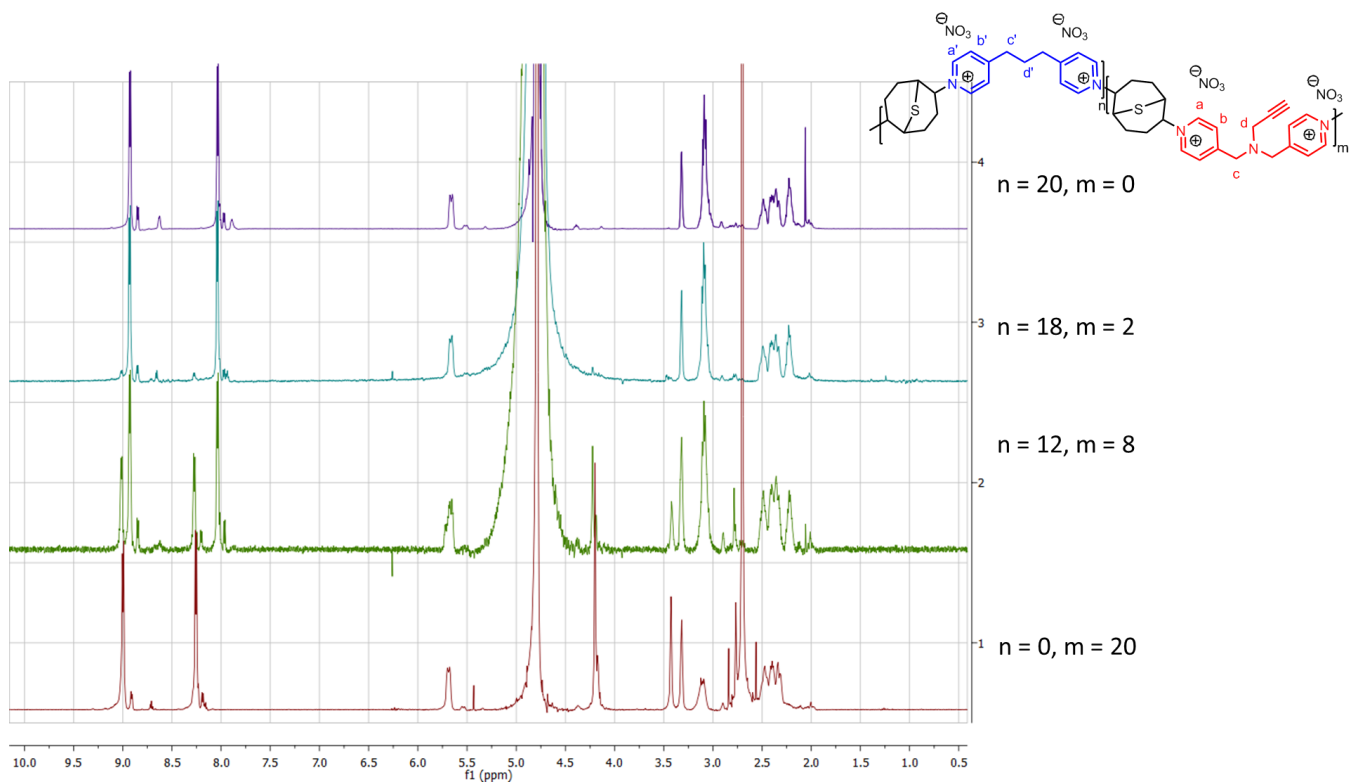
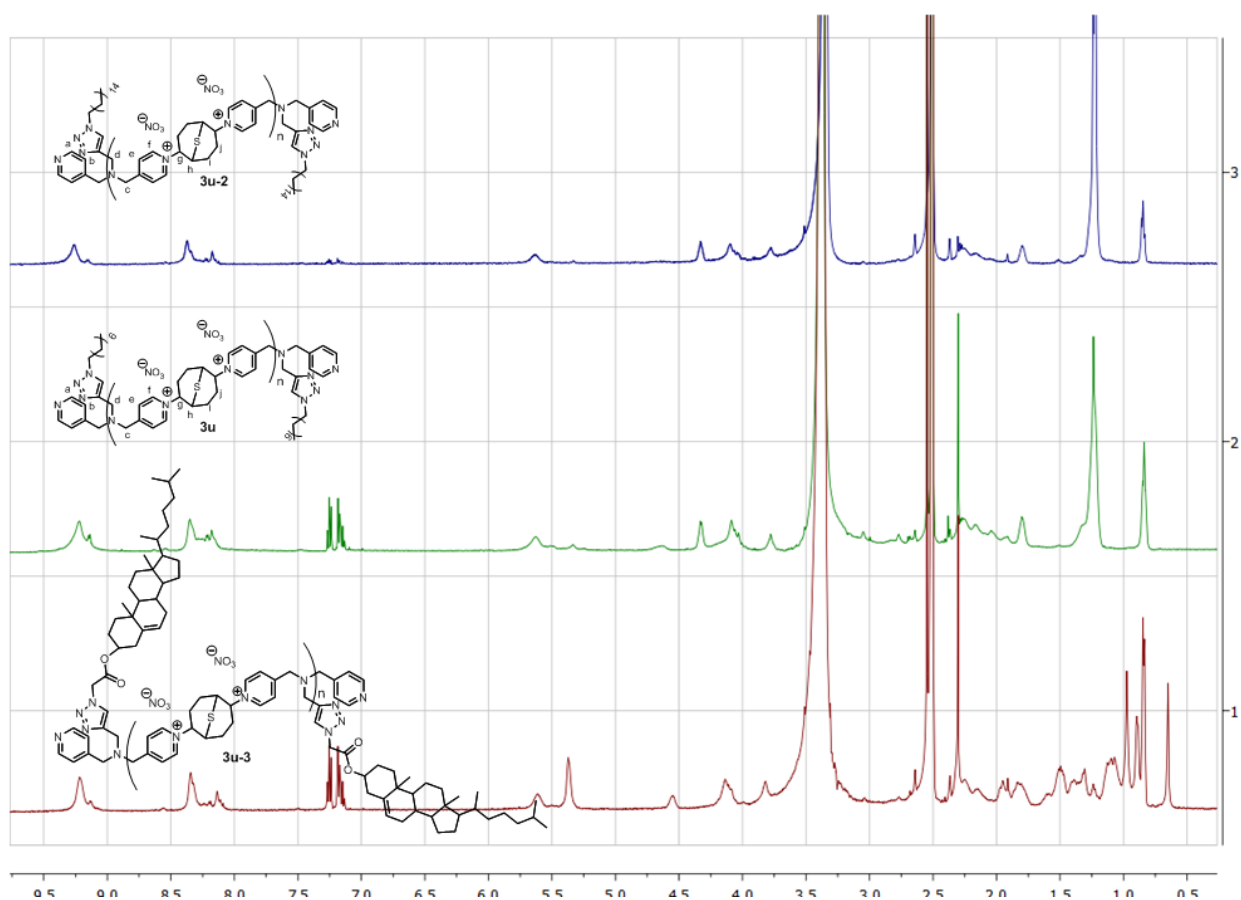












## References

1. Kumariya, R.; Sood, S. K.; Rajput, Y. S.; Saini, N.; Garsa, A. K. *Biochim. Biophys. Acta - Biomembranes* **2015**, *1848*, 1367-1375.
2. Nuri, R.; Shprung, T.; Shai, Y. *Biochim. Biophys. Acta - Biomembranes* **2015**, *1848*, 3089-3100.
3. Campos, M. A.; Vargas, M. A.; Regueiro, V.; Llopart, C. M.; Alberti, S.; Bengoechea, J. A. *Infect. Immun.* **2004**, *72*, 7107-7114.
4. Henderson, J. C.; Fage, C. D.; Cannon, J. R.; Brodbelt, J. S.; Keatinge-Clay, A. T.; Trent, M. S. *ACS Chem. Biol.* **2014**, *9*, 2382-2392.
5. Guina, T.; Yi, E. C.; Wang, H. L.; Hackett, M.; Miller, S. I. *J. Bacteriol.* **2000**, *182*, 4077-4086.
6. McPhee, J. B.; Lewenza, S.; Hancock, R. E. W. *Mol. Microbiol.* **2003**, *50*, 205-217.
7. Georg, M.; Maudsdotter, L.; Tavares, R.; Jonsson, A. B. *Cellular Microbiol.* **2013**, *15*, 1938-1954.
8. Oguri, T.; Yeo, W. S.; Bae, T.; Lee, H. *Antimicrob. Agents Chemother.* **2016**, *60*, 2222-2231.
9. Hong, J.; Hu, J. Y.; Ke, F. *Antimicrob. Agents Chemother.* **2016**, *60*, 6067-6075.
10. Wang, Z.; Bie, P. F.; Cheng, J.; Lu, L.; Cui, B. Y.; Wu, Q. M. *Sci. Rep.* **2016**, *6*.
11. Jennings, M. C.; Minbiole, K. P. C.; Wuest, W. M. *ACS Infect. Dis.* **2015**, *1*, 288-303.
12. Layman, J. M.; Borgerding, E. M.; Williams, S. R.; Heath, W. H.; Long, T. E. *Macromolecules* **2008**, *41*, 4635-4641.
13. Liu, S.; Ono, R. J.; Wu, H.; Teo, J. Y.; Liang, Z. C.; Xu, K.; Zhang, M.; Zhong, G.; Tan, J. P.; Ng, M.; Yang, C.; Chan, J.; Ji, Z.; Bao, C.; Kumar, K.; Gao, S.; Lee, A.; Favre, M.; Dong, H.; Ying, J. Y.; Li, L.; Fan, W.; Hedrick, J. L.; Yang, Y. Y. *Biomaterials* **2017**, *127*, 36-48.
14. Neugebauer, J. M. *Meth. Enzymol.* **1990**, *182*, 239-253.
15. Lienkamp, K.; Madkour, A. E.; Musante, A.; Nelson, C. F.; Nüsslein, K.; Tew, G. N. *J. Am. Chem. Soc.* **2008**, *130*, 9836-9843.
16. Siedenbiedel, F.; Tiller, J. C. *Polymers* **2012**, *4*, 46.
17. Malanovic, N.; Lohner, K. *Pharmaceuticals* **2016**, *9*, 59.
18. Jennings, M. C.; Buttar, B. A.; Minbiole, K. P. C.; Wuest, W. M. *ACS Infect. Dis.* **2015**, *1*, 304-309.
19. Silverman, J. A.; Oliver, N.; Andrew, T.; Li, T. *Antimicrob. Ag. Chemother.* **2001**, *45*, 1799-1802.
20. Gallo, R. L.; Hooper, L. V. *Nature Rev. Immunol.* **2012**, *12*, 503-516.
21. Costa, F.; Carvalho, I. F.; Montelaro, R. C.; Gomes, P.; Martins, M. C. L. *Acta Biomater.* **2011**, *7*, 1431-1440.
22. Han, J. H.; Floros, J. D. *J. Plastic Film & Sheeting* **1997**, *13*, 287-298.
23. Cha, D. S.; Chinnan, M. S. *Crit. Rev. Food Sci. Nutr.* **2004**, *44*, 223-237.
24. Page, K.; Wilson, M.; Parkin, I. P. *J. Mat. Chem.* **2009**, *19*, 3819-3831.
25. Siedenbiedel, F.; Tiller, J. C. *Polymers* **2012**, *4*, 46-71.
26. Kugler, R.; Bouloussa, O.; Rondelez, F. *Microbiol.-Sgm* **2005**, *151*, 1341-1348.
27. Lichter, J. A.; Van Vliet, K. J.; Rubner, M. F. *Macromolecules* **2009**, *42*, 8573-8586.
28. Lichter, J. A.; Rubner, M. F. *Langmuir* **2009**, *25*, 7686-7694.